

**JAERI-Review**

**94-006**



**IS PROCESS FOR THERMOCHEMICAL HYDROGEN  
PRODUCTION**

**November 1994**

**Kaoru ONUKI, Hayato NAKAJIMA, Ikuo IOKA  
Masatoshi FUTAKAWA and Saburo SHIMIZU**

**日本原子力研究所  
Japan Atomic Energy Research Institute**

本レポートは、日本原子力研究所が不定期に公開している研究報告書です。

入手の問合わせは、日本原子力研究所技術情報部情報資料課（〒319-11 茨城県那珂郡東海村）あて、お申し込みください。なお、このほかに財団法人原子力弘済会資料センター（〒319-11 茨城県那珂郡東海村日本原子力研究所内）で複写による実費領布をおこなっております。

This reports are issued irregularly.

Inquiries about availability of the reports should be addressed to Information Division Department of Technical Information, Japan Atomic Energy Research Institute, Tokaimura, Naka-gun, Ibaraki-ken 319-11, Japan.

© Japan Atomic Energy Research Institute, 1994

編集兼発行 日本原子力研究所  
印刷 ニッセイエプロ株式会社

IS Process for Thermochemical Hydrogen Production

Kaoru ONUKI, Hayato NAKAJIMA, Ikuo IOKA  
Masatoshi FUTAKAWA and Saburo SHIMIZU

Department of High Temperature Engineering  
Tokai Research Establishment  
Japan Atomic Energy Research Institute  
Tokai-mura, Naka-gun, Ibaraki-ken

(Received October 11, 1994)

The state-of-the-art of thermochemical hydrogen production by IS process is reviewed including experimental data obtained at JAERI on the chemistry of the Bunsen reaction step and on the corrosion resistance of the structural materials. The present status of laboratory scale demonstration at JAERI is also included.

The study on the chemistry of the chemical reactions and the products separations has identified feasible methods to function the process. The flowsheeting studies revealed a process thermal efficiency higher than 40% is achievable under efficient process conditions. The corrosion resistance of commercially available structural materials have been clarified under various process conditions. The basic scheme of the process has been realized in a laboratory scale apparatus.

R&D requirements to proceed to the engineering demonstration coupled with HTTR are briefly discussed.

Keywords: Thermochemical Method, Hydrogen Production, IS Process, Bunsen Reaction, Sulfuric Acid, Hydrogen Iodide, Phase Separation, Flowsheeting, Structural Materials, Laboratory Scale Demonstration, HTTR, HENDEL.

熱化学水素製造法 IS プロセスの研究開発

日本原子力研究所東海研究所高温工学部

小貫 薫・中島 隼人・井岡 郁夫

二川 正敏・清水 三郎

(1994年10月11日受理)

熱化学水素製造法 IS プロセスに関して、原研及び各国の研究機関で進められてきた研究開発の成果をとりまとめた。

これまでに、要素反応及び生成物分離方法の研究から、いくつかの実行可能なプロセス条件が見いだされている。それらの知見に基づいたプロセスフローシートの検討から、効果的な排熱回収を組み込んだ最適なプロセス条件の下で40 % を越えるプロセス熱効率の期待できることが示された。装置材料に関して、1000 時間程度の耐食試験により腐食性の強いプロセス環境に対する市販材料の耐食性を明らかにした。現在、プロセスの全基本工程を組み込んだ実験室規模プラントの運転試験により、閉サイクル運転条件の検討を進めている。

HTTR 接続試験に進むために必要な研究開発について議論した。

## Contents

1. Introduction .....	1
2. Overview of IS Process .....	3
3. Chemistry of the Process .....	6
3.1 Bunsen Reaction Step .....	6
3.2 Hydrogen Iodide Decomposition Step .....	10
3.3 Sulfuric Acid Decomposition Step .....	15
4. Process Flowsheeting .....	18
5. Structural Materials .....	20
5.1 Bunsen Reaction Step .....	20
5.2 Hydrogen Iodide Decomposition Step .....	21
5.3 Sulfuric Acid Decomposition Step .....	23
6. Laboratory Scale Demonstration .....	25
7. Future Works .....	28
7.1 Process Chemistry & Flowsheeting .....	28
7.2 Structural Materials .....	29
7.3 Process Demonstration .....	29
Acknowledgments .....	31
References .....	32

## 目 次

1. 序 .....	1
2. IS プロセスの概要 .....	3
3. 要素反応工程の化学 .....	6
3.1 ブンゼン反応工程 .....	6
3.2 ヨウ化水素分解工程 .....	10
3.3 硫酸分解工程 .....	15
4. プロセスフローシート .....	18
5. 装置材料 .....	20
5.1 ブンゼン反応工程 .....	20
5.2 ヨウ化水素分解工程 .....	21
5.3 硫酸分解工程 .....	23
6. 実験室規模プロセス実証試験 .....	25
7. 今後の課題 .....	28
7.1 要素反応及びフローシート .....	28
7.2 装置材料 .....	29
7.3 プロセス実証試験 .....	29
謝 辞 .....	31
参考文献 .....	32

## 1. Introduction

Since the oil crisis in 70's, a number of alternative energy resources and technologies have been studied. The need for such new energies has become emphasized by the global environmental issues widely recognized in recent years. Nuclear energy and hydrogen is a promising candidate for such an new primary and secondary energy, respectively. "Thermochemical method" for hydrogen production offers a technology with which nuclear energy is transformed into hydrogen, the new energy carrier.

In order to produce a practically interesting amount of hydrogen through the direct thermal decomposition of water, one needs a heat source of temperature higher than a few thousand Kelvin. On the contrary, by a chemical cycle composed of endothermic and exothermic chemical reactions, it is possible, in principle, to decompose water with heat of temperature far lower than that. This method, which is called "thermochemical hydrogen production", was first proposed by Funk[1] and an actual example of the "thermochemical process" was first proposed by the researchers of CEC, JRC Ispra establishment in early 70's[2].

Since then, a number of thermochemical processes have been proposed assuming, in most cases, High Temperature Gas-Cooled Reactor (HTGR) as the heat source by which nuclear heat at temperature of ca.1270K is available. Through studies on the chemical reactions and products separations, structural materials, and flowsheeting, a few promising processes were selected until mid-80's[3].

After mid-80's, unfortunately, activities in Europe and in North America became slowing down in accordance with the slowing down of their HTGR projects. However, the importance of the technology has been and will be unchanged considering the problems accompanied with the use of fossil resources, i.e., the limited amount of the deposits and the effects on the global environment. In Japan, because of the lack of domestic energy resources and the increasing requirements for cleaner fuels, research works on the thermochemical hydrogen production have been encouraged and continued in many academic institutions[4] and in Japan Atomic Energy Research Institute (JAERI)[5].

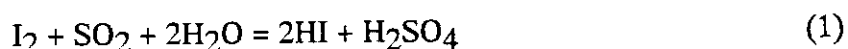
In this report, the present status of R&D on one version of "Iodine-Sulfur (IS) process" is reviewed including experimental data obtained at JAERI. The process was first proposed by General Atomics (GA) in early 70's[6], and the R&D has

been carried out at GA, Rheinische-Westfälische Technische Hochschule (RWTH) Aachen, University of Montreal, JAERI etc. In chapter 2, the outline of the process R&D is briefly summarized. In chapter 3, the so far obtained knowledge on the chemistry of the chemical reactions and the products separations is described. In chapter 4, the process thermal efficiencies estimated under various process conditions are summarized. In chapter 5, the results of the screening tests for the corrosion resistant structural materials are presented. In chapter 6, present status of the process demonstration in laboratory scale is described. Chapter 7 concerns the future works in relation to the R&D requirements for coupling the process with High Temperature Engineering Test Reactor (HTTR) which is under construction at JAERI.



## 2. Overview of IS Process

Iodine-Sulfur process (IS process) is composed of the following three chemical reactions.



Here, reaction (1) is known as "Bunsen reaction", where gaseous sulfur dioxide reacts with iodine and water producing an aqueous solution of hydriodic acid and sulfuric acid. Thermal decomposition of hydrogen iodide (2) and that of sulfuric acid (3) produces hydrogen and oxygen, respectively. By carrying out these three reactions sequentially, as a net material balance of the process, water can be decomposed into hydrogen and oxygen.

The high temperature nuclear heat supplied by HTGR is utilized for the heat of reaction of the sulfuric acid decomposition which proceeds endothermically at temperature range of 1020–1170K. On the contrary, the Bunsen reaction proceeds exothermically at 290–370K. Therefore, IS process works like a chemical engine which absorbs high temperature nuclear heat and produces high quality chemical energy, hydrogen, and waste heat.

In order to develop the process, research should be carried out in the following fields,

- (a) Chemistry of each reaction step concerning reaction equilibrium, reaction rate and products separation,
- (b) Process flowsheeting,
- (c) Structural materials,
- (d) Process demonstration.

Studies on these fields have so far been carried out interconnectedly along with the extension of the knowledge on the chemistry of the reaction steps.

Concerning the chemistry of the reaction and the separation, there has been two main problems to be overcome. One is how to separate the hydriodic acid and sulfuric acid produced by the Bunsen reaction. The other is how to carry out the hydrogen iodide decomposition reaction of which, in the gaseous phase, the reaction equilibrium is unfavorable to the products. Many variations have been proposed of the process to overcome these difficulties such as to carry out the Bunsen reaction in an electrochemical cell[7] or to add chemical sub cycles[8][9][10] etc.

A most promising scheme on the separation problem was proposed by the researchers of GA[6]. They found that the mixed acid solution produced by the Bunsen reaction separated spontaneously into two liquid phases in the presence of excess amount of iodine. The heavier phase is mainly composed of HI, I<sub>2</sub>, and H<sub>2</sub>O, and is called "HI<sub>x</sub>" solution. The main components of the lighter phase are H<sub>2</sub>SO<sub>4</sub> and H<sub>2</sub>O. The phenomena offered an easy way of separating the hydriodic acid and the sulfuric acid. Fig.2.1 shows a simplified scheme of IS process featuring the liquid-liquid phase separation. Here, a distillation is included to separate hydriodic acid from iodine to facilitate the decomposition of hydrogen iodide. GA has made a lot of achievement in its R&D. At present, JAERI is also pursuing the same scheme.

As for the decomposition of hydrogen iodide, some innovative methods have been proposed so far, by GA, RWTH etc. The proposed methods are promising from the standpoint of the process thermal efficiency though most of the process conditions employed are quite severe for the structural materials of the reactor vessels.

Preliminary flowsheeting studies carried out at GA, RWTH etc. showed the "process thermal efficiency" of 40-50% can be expected under optimum operating conditions and assuming maximum heat recovery. Here, the thermal efficiency is defined as the ratio of the Higher Heating Value (HHV) of hydrogen to the net energy input for the process.

Since the process utilizes corrosive chemicals such as sulfuric acid and halogen, the selection of the structural materials for the reactor vessels constitutes an important part of the process R&D. So far, screening tests have been carried out using test pieces of commercially available materials at many research institutions. In general, many commonly used metals have been found to show corrosion resistance in the gaseous process environments. On the contrary, in the hot acidic solution environments, the number of commercial materials which show corrosion resistance is limited.

A laboratory scale demonstration has been carried out, at GA and also at JAERI, to show the continuous production of hydrogen and to examine the process characteristics under recycle use of the process fluids.

In conclusion, the process has been shown to be feasible and efficient in principle. In order to proceed to the engineering demonstration coupled with HTTR, extensive studies are required mainly in the following fields.

a) Process Chemistry & Flowsheeting

Establishment of the method for processing of the  $\text{HI}_x$  solution, which should be efficient from the view point of thermal efficiency and offer a mild environment for the reactor materials as well.

b) Structural Materials

Study on the effect of the environments on the mechanical properties. Concerning the concentrator and the boiler of sulfuric acid, the  $\text{HI}_x$  distillation column, extensive research and development of the corrosion resistant materials is required. Study on the reactor design considering the structural integrity.

c) Process Demonstration

Laboratory scale demonstration to show the scientific feasibility of the process should be followed by the demonstration using metallic reactors which aims to acquire engineering data. Then, a large scale experiment using an helium loop (HENDEL) is necessary to demonstrate the long time stability of the plant operation.

### 3. Chemistry of the Process

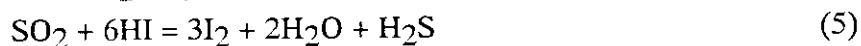
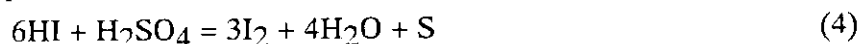
Knowledge on the chemistry of the reactions and the related separations is reviewed in the order of the Bunsen reaction step, the thermal decomposition of hydrogen iodide step and the thermal decomposition of sulfuric acid step. Experimental data on the Bunsen reaction and the following processing of the solution is included which has been obtained at JAERI in relation to the laboratory scale demonstration experiments which will be described in chapter 6.

#### 3.1 Bunsen Reaction Step

In this step, hydriodic acid and sulfuric acid are produced by the Bunsen reaction, and separated by the phase separation. In the following, possible side reactions, reaction equilibrium, reaction rate, and product separation will be discussed.

##### 3.1.1 Stability of the Product Solution

The reaction is carried out as a sulfur dioxide gas absorption reaction by an aqueous solution of iodine. From the viewpoint of energy economics of IS process, high acid concentration is desirable for the product solution. However, unfavorable side reactions such as sulfur formation are known to occur in the concentrated mixture of hydriodic acid and sulfuric acid. The following reaction equation has been proposed for the formation of sulfur and hydrogen sulfide[11].



Kumagai et al. of National Chemical Laboratory for Industry (NCLI) examined the stability of the mixed acid at 343K in the absence of iodine and in the concentration range of  $[\text{H}^+] = 2-8 \text{ mol/kg-H}_2\text{O}$  and  $2[\text{H}_2\text{SO}_4]/[\text{HI}] = 0.2-1.0$ [12]. It is reported that the sulfur formation according to the equation (4) was observed when the proton concentration was higher than  $4 \text{ mol/kg-H}_2\text{O}$ , which depended little on the molar ratio of the acids.

We have studied the Bunsen reaction at 333K varying the initial composition of the reactants[13]. In case of equal mixture of iodine and sulfur dioxide, the sulfur formation was observed when the mole fraction of reactant sulfur dioxide was higher than 0.0255. On the other hand, in case of the reactant molar ratio of  $[\text{I}_2]/[\text{H}_2\text{O}] = 0.226$  where the products separated into two liquid phases, the sulfur formation was observed when the mole fraction of reactant  $\text{SO}_2$  was higher than 0.04. These results mean the stability of the concentrated mixed acid increases un-

der two phase separation condition which is realized in the presence of excess iodine.

In the following sections, the reaction equilibrium, the reaction rate, and the phase equilibrium are discussed under the condition of no sulfur formation.

### 3.1.2 Reaction Equilibrium

The thermodynamic data of the species in the  $\text{H}_2\text{O}$ - $\text{HI}$ - $\text{H}_2\text{SO}_4$ - $\text{I}_2$  system is not available at present. However, practically useful information has been obtained on the yield of acids as a function of reactant composition and temperature.

Experiments were performed by feeding a gaseous mixture of sulfur dioxide (18mol%) and nitrogen into a prescribed amount of mixture of iodine and water until the sulfur dioxide gas appeared in the tail gas. Then, an inert gas was bubbled in the product solution to remove the dissolved sulfur dioxide until its vapor pressure became equal to or lower than 50 Pa. The observed relationship between the amount of sulfur dioxide absorbed and the weight ratio of the absorbents,  $\text{I}_2/\text{H}_2\text{O}$ , is shown in Fig.3.1 in the temperature range of 298–363K. The appearance of the product changed with increasing the ratio of  $\text{I}_2/\text{H}_2\text{O}$  as follows,

- transparent one phase solution (region A),
- brown colored one phase solution (region B),
- brown colored two phase solution (region G), and
- brown colored two phase solution with solid iodine (region N).

It was confirmed, from a material balance calculation based on the chemical analysis data of the products and the stoichiometry of reaction (1), that the reaction proceeded quantitatively without side reaction. The product solution was found to be stable for more than a week. Hence, it is considered that the chemical equilibrium of the reaction (1) under sulfur dioxide pressure of ca.50 Pa was achieved in the product solution.

From Fig.3.1, the followings can be pointed out.

- (a) At a constant temperature, the yield of acids per unit amount of water increases with increasing the iodine activity until it reaches that of iodine saturated solution.
- (b) The reaction equilibrium is little dependent on the temperature within the range of 298–363K.
- (c) The acid concentration in the product under iodine saturation increases

with increasing temperature owing to the increase of the iodine solubility.

The effect of hydriodic acid concentration in the absorbing mixture on the sulfur dioxide absorption was further studied at 298K. As expected, the absorbable amount of sulfur dioxide decreased with increasing the initial concentration of the hydriodic acid. An interesting relationship was found between the molar ratio of total iodine atom to iodide ion in the equilibrium mixture,  $X$ , and the initial molar fraction of iodine in the mixture of iodine and water,  $\{I_2/(I_2+H_2O)\}$ . As shown in Fig.3.2, the relationship between the two variables could be expressed by a straight line irrespective of the initial composition of hydriodic acid, so long as the initial molar fraction of iodine is larger than ca.0.05. The relationship could be approximated by the following equation.

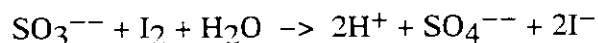
$$X = 22.1x\{I_2/(I_2+H_2O)\} + 1 \quad (6)$$

Little is known about the effect of sulfur dioxide partial pressure on the equilibrium. Norman et al.[14] estimated the yield of the acids was not sensitive to it. They reported the yield of sulfuric acid which was obtained by feeding sulfur dioxide of 1 atmospheric pressure[15]. The reported value is plotted in Fig.3.1, which lies close to the absorption limit curve obtained in the present experiments.

### 3.1.3 Reaction Rate

The reaction (1) is a reversible reaction as seen above. The following data is available on the rate of the forward reaction.

Eigen et al.[16] measured the reaction rate at 293K by a stopped-flow method, and obtained the following results. In a neutral solution, a following reaction dominates,



and the bimolecular( $SO_3^{--}$  &  $I_2$ ) reaction rate is higher than  $10^6 \text{ l mol}^{-1} \text{ s}^{-1}$ . On the other hand, under the condition of  $0 < \text{pH} < 1$ , the reaction intermediate changes from  $SO_3^{--}$  to  $H_2SO_3$  and the overall bimolecular rate constant is  $3 \times 10^5 \text{ l mol}^{-1} \text{ s}^{-1}$ . Further, under the condition of  $\text{pH} < 1$  and iodine concentration  $> 0.05 \text{ mol l}^{-1}$ , the reaction rate is quasi-monomolecular concerning the sulfur dioxide concentration and its rate constant lies between  $10^2 - 10^3 \text{ s}^{-1}$ .

Kumagai et al.[12] confirmed that the rate of sulfur dioxide absorption is independent of iodine concentration under the reaction condition of iodine concentra-

tion: 0–0.4 mol kg<sup>-1</sup>, and proton concentration: 1.8–3.5 mol kg<sup>-1</sup>.

Concerning the temperature effect on the reaction rate, no quantitative measurement has been reported so far. Also, since no quantitative data is available at present on the reaction rate of the backward reaction, the reaction rate near equilibrium composition is not yet clear.

### 3.1.4 Products Separation

The effect of iodine concentration and temperature on the phase separation is shown in Fig.3.3 and Fig.3.4, respectively. Here, the ordinate denotes the molar ratio of H<sub>2</sub>SO<sub>4</sub>/HI in the heavier phase. At constant temperature, higher iodine concentration is effective for the better separation. At constant composition, the better separation can be achieved with lowering the temperature.

Therefore, the better separation is expected in an iodine saturated solution at low temperature. But, since the iodine solubility increases with temperature, the temperature dependence of the separation behavior under iodine saturation is not straightforward as shown in Fig.3.5. However, since the effect of iodine solubility dominates the separation factor at temperatures above ca. 283K as seen in the figure, the better separation can be seen with increasing the temperature under iodine saturation.

There are two other variables, the concentrations of the acids, which may affect the separation phenomena. We have measured the density of the HI–I<sub>2</sub>–H<sub>2</sub>SO<sub>4</sub>–H<sub>2</sub>O solution under iodine saturation at 294K as a function of the composition[5]. The phase separation occurred in the region of X(H<sub>2</sub>O) lower than 0.92 at 294K. Here, X(H<sub>2</sub>O) denotes the molar ratio of H<sub>2</sub>O/(HI+H<sub>2</sub>SO<sub>4</sub>+H<sub>2</sub>O). With further increase of the acid concentration, the iodine solubility increased resulting in the increase of the density of heavier phase. It was found that the densities of the phase separated solutions depended largely on the concentration of acids and little on the molar ratio of the acids. This indicates that the ratios of water to acid in both phases have a similar value. Considering the effect of iodine concentration on the separation factor discussed above, the better separation is expected with higher concentration of acids.

Concerning the stability of the solution at 294K, there was no sign of side reaction so long as X(H<sub>2</sub>O) was higher than 0.86. In the more concentrated solution a

production of hydrogen sulfide was observed. The value of 0.86 for  $X(\text{H}_2\text{O})$  is close to the stability limit against sulfur formation at 333K[13].

From these results, the following practically useful information can be pointed out,

- (a) at constant temperature, the best separation can be expected at acid concentration close to the stability limit under iodine saturation,
- (b) at the temperature of higher than 283K, the better separation can be achieved with increasing the temperature.

The liquid-liquid phase separation phenomena in the product solution of the Bunsen reaction, where the molar ratio of HI to  $\text{H}_2\text{SO}_4$  is 2, was studied by Norman et al.[14][15][17]. They measured the yield of sulfuric acid in the lighter phase as a function of the reactant ratio of iodine to water. They discussed on the "best" reaction condition using a figure of merit which was defined as the yield of  $\text{H}_2\text{SO}_4$  divided by the heat required to purify it. It was concluded that there are two possibilities for the "best" reaction condition, i.e.,

- (a) near iodine saturation at 368K,
- (b) using ca.25% more iodine than (a) and at >388K.

We have measured the separation factor of the mixed acid solution obtained by the Bunsen reaction under iodine saturation. Fig.3.6 shows the results, where the measured separation factor in the  $\text{HI}_x$  phase at 368K is consistent with that reported by Norman et al.

Considering the above mentioned knowledge, a possibility can be pointed out on the optimum separation condition. Although the best separation is expected in the composition close to the stability limit, the acid concentration obtainable by the Bunsen reaction is lower than the limiting concentration for side reactions as discussed above. Therefore, utilization of such a high acid composition only in the separation process might be beneficial to the process efficiency.

### 3.2 Hydrogen Iodide Decomposition Step

This step produces hydrogen, and is composed of the purification of the  $\text{HI}_x$  solution from the Bunsen reaction step, the distillation of the purified  $\text{HI}_x$  solution, the decomposition of hydrogen iodide, and the separation of hydrogen from the reaction mixture.

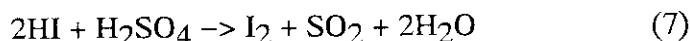


### 3.2.1 Purification of the $\text{HI}_x$ solution

The  $\text{HI}_x$  solution from the Bunsen reaction step contains a small amount of  $\text{H}_2\text{SO}_4$ . The sulfuric acid concentration in the  $\text{HI}_x$  depends on the separation condition. In the case of the Bunsen reaction products under iodine saturation at 368K, the molar ratio of  $\text{H}_2\text{SO}_4/(\text{HI}+\text{H}_2\text{SO}_4)$  in the  $\text{HI}_x$  is only 0.005 as shown in Fig.3.6. However, if the solution as produced is fed to the distillation column, the sulfur is formed at the top of the column according to eq.(4) by which 6 moles of HI are consumed per 1 mol of  $\text{H}_2\text{SO}_4$ . Therefore, any sulfuric acid should be removed from the  $\text{HI}_x$  solution before its distillation and recycled in IS process.

Concerning the  $\text{HI}_x$  solution made by the Bunsen reaction at 368K under iodine saturation, Norman et al.[18] reported that the sulfur formation in the downstream process could be apparently avoided by scrubbing the solution with nitrogen gas bubbling. The observed effect was speculated due to

- (a) removal of the dissolved sulfur dioxide, and
- (b) reverse reaction of the Bunsen reaction,



which proceeds with the progress of sulfur dioxide removal.

In order to confirm the sulfur balance of the treatment, we have carried out experiments using  $\text{HI}_x$  solution having maximum acid concentration obtainable by the Bunsen reaction under iodine saturation at room temperature. The solution was moderately heated up under nitrogen gas bubbling, and the effluent was measured by an IR spectrometer and/or titration after absorbing it in an iodine–water solution. The solution was vigorously stirred throughout the experiments. With heating up the solution, water distilled at first and then sulfur dioxide began to distill at ca.353K. The distilling rate increased with increasing temperature, and above 373K the distillate formed a mixed acid in the cold part of the downstream. The phenomena can be explained by the Bunsen reaction which occurred as the iodine concentration in the distillate increased. The measured sulfur balance showed that there exists a condition where complete separation of the acids by reaction (7) is possible without sulfur formation. Vigorous mixing, moderate liquid temperature (ca.373K), and large gas flow rate were effective to shorten the operation time and to avoid the sulfur formation.

The separated sulfur dioxide can be recovered by feeding it to the Bunsen reac-

tion step. Concerning the purification method, parametric study is further required for determining the optimum condition. Finally, it can be pointed out that, considering the suitable conditions mentioned above, the removal of sulfur dioxide may be able to be carried out under reduced pressure.

### 3.2.2 Distillation of the $\text{HI}_x$ solution

The purpose of the distillation is to separate iodine from hydrogen iodide to facilitate the decomposition of hydrogen iodide. The simplest one is the distillation under atmospheric pressure (conventional distillation), by which hydriodic acid of azeotropic composition (57wt% HI) can be obtained. However, it consumes a lot of energy, and less energy consuming method is desired.

Researchers of GA examined the effect of concentrated phosphoric acid addition to the  $\text{HI}_x$  solution[17]. They found that

- (a) the solubility of iodine in concentrated phosphoric acid is very low, and
- (b) the azeotrope of  $\text{HI}-\text{H}_2\text{O}$  system disappears in the presence of  $\text{H}_3\text{PO}_4$ , when the mole fraction of  $\text{H}_3\text{PO}_4$  is higher than 85% (HI free base).

Based on the findings and the related phase equilibrium data of the system[14], i.e., mutual solubility of two liquid phases in  $\text{H}_3\text{PO}_4-\text{HI}-\text{I}_2-\text{H}_2\text{O}$  system and the vapor-liquid equilibrium, a process was proposed composed of a counter current column for the iodine separation, an extractive distillation column for the hydrogen iodide separation, and a multistage evaporator for phosphoric acid reconcentration[18]. In this case, pure hydrogen iodide can be obtained as the distillate, although the vaporization of water is also required to reuse the phosphoric acid.

Researchers of RWTH Aachen proposed a reactive distillation where hydrogen iodide is decomposed at the upper part of the column. They measured the vapor pressure of the  $\text{HI}_x$  solution with molar ratio of  $\text{HI}/\text{H}_2\text{O}$  ranging 0–0.19 in the temperature range of 393–573K[19][20], and found the following features of the vapor-liquid equilibrium.

- (a) The vapor pressure minima, which connects the composition of  $\text{HI}/\text{H}_2\text{O}$  azeotrope and pure iodine in the phase diagram, depends little on temperature where iodine fraction is high. Whereas, under low iodine fraction, it moves toward higher water composition as temperature increases.
- (b) When the composition is located in the HI-rich region compared to that of vapor pressure minima and the fraction of iodine is low, the decomposi-

tion of hydrogen iodide proceeds and the reaction equilibrium should be taken into account at temperature higher than ca.453K.

The measured vapor pressure data were correlated with the composition using a modified NRTL equation[21]. Using thus obtained vapor-liquid equilibrium data, they designed a distillation column operated under pressure of 2.22MPa[22]. According to the design, this column produces hydrogen directly from the  $\text{HI}_x$  solution and the thermal burden is less compared to that of the phosphoric acid process. However, since the circulation of  $\text{HI}_x$  is quite large, large internal heat exchangers are required.

The distillation of  $\text{HI}_x$  solution is one of the most energy consuming steps in IS process. The two methods mentioned above present an possibility of reducing the thermal burden. However, because of the strong corrosive conditions, these ideas were not yet demonstrated in the proposed conditions.

### 3.2.3 Reaction Equilibrium

The gas phase equilibrium conversion ratio of Reaction (2) lies between 15–21% in the temperature range of 500–700K as shown in Fig. 3.7. The low conversion ratio results in the increase of the circulating amounts of the process fluids, which lowers the process thermal efficiency and enlarges the reactor size. Therefore, methods have been explored to attain higher once-through conversion, by removing one of the products from the reaction zone selectively.

One method is to use an adsorbent which selectively adsorbs iodine. Researchers of GA[23] and also of NCLI[24] noticed, in their study on the catalytic decomposition of gaseous hydrogen iodide, that some catalysts act as the iodine adsorbent. It has been demonstrated at NCLI and at JAERI that, with Pt catalyst supported on activated carbon, the once-through conversion up to 70–75% was possible at 473K[24][25]. Although this concept has been proven to work, the adsorbent saturated with iodine should be reactivated by heating it to ca. 570K under reduced pressure for reuse. The energy requirement for the reactivation seems relatively large.

Use of perm-selective membranes was discussed by Itoh et al.[26]. The simulation results showed the possibility of obtaining higher once-through conversion than equilibrium one using micropore membrane. To realize the concept, however,

development of the membrane with high selectivity and permeation rate is required.

Researchers of GA discussed the equilibrium conversion obtainable in the reactor where the two phases (liquid and vapor) of hydrogen iodide coexisted[23]. Based on the study on the vapor-liquid equilibrium and using the reaction equilibrium data, the gas phase partial pressures of HI, I<sub>2</sub>, and H<sub>2</sub> were determined as a function of HI distribution ratio between the vapor and the liquid phases. From the obtained relationship, the conversion ratio of hydrogen iodide was calculated in the temperature range of 363–423K. The results showed that, from viewpoint of equilibrium, it was possible to attain higher conversion ratio of HI than that expected in the homogeneous gas phase reaction. It was calculated the equilibrium conversion exceeded 50% at 393K, and the effect was attributed to the low volatility of iodine. An attractive point with this method is that the compression of hydrogen can be avoided for supplying to the pipe line, since the reactor is operated under high pressure.

#### 3.2.4 Reaction Rate

The homogeneous gas phase decomposition reaction of hydrogen iodide is a reversible reaction. The reaction rate is known to be expressed by[27],

$$-d[\text{HI}]/dt = k_1[\text{HI}]^2 - k_2[\text{H}_2][\text{I}_2]. \quad (8)$$

Fig.3.7 shows the conversion of HI calculated using the compiled rate constants[28] as functions of time and temperature. Since the reaction equilibrium hardly depends on temperature and the decomposition environment is strongly corrosive, a low temperature operation is desirable. However, as seen in the figure, the reaction rate is very slow at temperature lower than 700K. Therefore, catalysts are necessary to meet the requirement.

Researchers of NCLI surveyed the catalytic activity of transition metal elements or compounds using a variety of supports, such as alumina, silica, zeolite, active carbon, teflon etc.[29]. They found that platinum group metal showed high catalytic activity and the combination of Pt with active carbon support (Pt/C) showed the highest activity. Apart from the noble metals, active carbon itself showed good catalytic activity. With Pt/C catalyst, it is reported that the equilibrium conversion could be reached within the contact time of 0.1 sec at 650–700K. Concerning Pt/C and active carbon catalysts, the kinetics of the contact reaction was found to be well represented by the following expression[30],

$$-kt = ax + (ax_e^2 + 2x_e - 1) \ln\{(x_e - x)/x_e\} / x_e + (x_e - 1)^2 \ln[(x_e - x)/\{x_e(ax_e x - 1)\}] / \{x_e(ax_e^2 + 1)\} \quad (9)$$

where  $x$ ,  $x_e$ , and  $t$  denotes conversion, equilibrium conversion, and time, respectively.  $k$  and  $a$  is constants related to the initial partial pressures and the adsorption coefficients of the reactants, respectively. With these kinetic investigation, it was clarified that at high temperature the active carbon suffered the water-gas reaction and at low temperature the reaction rate was strongly inhibited by iodine. They concluded that the suitable reaction temperature of the contact reaction lies between 550–700K.

Researchers of GA surveyed the catalysts suitable for the liquid phase decomposition reaction mentioned in section 3-2-3.[23]. It is reported that Platinum supported on  $\text{TiO}_2$ ,  $\text{ZrO}_2$  etc. showed catalytic activity. With these catalysts, conversion ratio of over 50% was demonstrated at 303K. It is claimed that the extrapolated reaction rate calculated with the aid of the activation energies measured for the catalyst system approached the engineering requirements at temperature of 403–423K. Concerning the concept, the use of liquid phase homogeneous catalyst was also considered[31].

### 3.2.5 Products Separation

The separation of hydrogen from other components can easily be carried out by cooling the reaction mixture down to 280–290K.

## 3.3 Sulfuric Acid Decomposition Step

In this step, the purification of the sulfuric acid phase solution, the concentration and the vaporization of the purified sulfuric acid, and the decomposition of sulfuric acid are carried out. Except the purification, the operations in this step are common in many thermochemical processes, which are usually termed as "Sulfur Family". So, the chemistry of the step has been relatively well studied.

### 3.3.1 Purification of the Sulfuric Acid

The sulfuric acid phase solution obtained in the Bunsen reaction step contains 40–50wt%  $\text{H}_2\text{SO}_4$  and small amounts of HI and  $\text{I}_2$ . The contamination level is similar to the case of HIX solution. The effect of these unseparated HI and  $\text{I}_2$  in the following treatments of sulfuric acid is not clear at present. But, according to our experience of the cyclic operation of laboratory scale plant, the direct vaporization of the contaminated sulfuric acid produced a black precipitate in the vaporizer. The

XRD analysis showed the precipitate was compounds of sulfur and iodine.

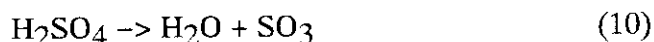
So, it seems necessary to separate the HI and I<sub>2</sub> from the sulfuric acid as much as possible. Fortunately, we have found the separation was possible in the same manner as in the case of HI<sub>x</sub> solution.

### 3.3.2 Concentration and Vaporization of the Sulfuric Acid

The required vapor-liquid equilibrium data for the treatment is available in commonly used data base. Recently, an extensive correlation result was published on the partial pressures and the enthalpies of H<sub>2</sub>O-H<sub>2</sub>SO<sub>4</sub> in the composition range up to 80 mol% H<sub>2</sub>SO<sub>4</sub> and the temperature range of 273K to 513K[32].

### 3.3.3 Reaction Equilibrium

The thermal decomposition of sulfuric acid proceeds in the following two steps.

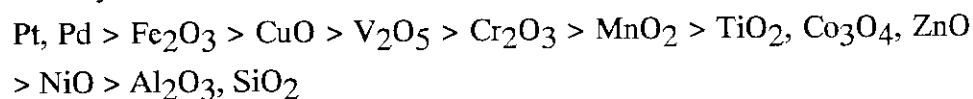


The reaction (10) proceeds at 670–770K, while the reaction (11) proceeds at 1020–1170K. The equilibrium conversion ratio of the latter reaction is shown in Fig.3.8 and Fig.3.9 as a function of initial SO<sub>3</sub> concentration and pressure, respectively[33]. As seen in the figures, the reaction equilibrium favors high temperature and low pressure conditions. Since the reaction step absorbs the nuclear heat which is supplied by the sensible heat of helium gas, the reaction condition will be determined considering the characteristics of both the chemical reaction and the heat source.

### 3.3.4 Reaction Rate

The reaction (10) proceeds spontaneously as a homogeneous gas phase reaction. On the contrary, the reaction (11) needs a catalyst. Many reports are available on the topics.

Researchers of Government Industrial Research Institute Osaka(GIRIO)[34], NCLJ[35], and GA[36] examined the catalytic activity of noble metals and of transition metal oxides. The results can be summarized in the following order of catalytic activity.



The reaction rates were reported on Pt and  $\text{Fe}_2\text{O}_3$  catalyst from GIRIO[34], Westinghouse Co.(WH)[37], and JAERI[33]. With the  $\text{Pt}/\text{Al}_2\text{O}_3$  catalyst, the decomposition reaction reached equilibrium at space velocity of  $20000 \text{ hr}^{-1}$  and 1153K. The reaction rate is apparently first order with  $\text{SO}_3$  concentration.

It is reported that the sulfate formation poisons the transition metal oxide catalyst[36]. The sulfate formation should therefore be considered in selecting metal oxide support for the noble metal catalysts as well .

Concerning the life of catalyst, GIRIO reported the activity of 3wt%  $\text{Fe}_2\text{O}_3/\text{Al}_2\text{O}_3$  had not changed after 1000 hr operation[34].

### 3.3.5 Products Separation

The separation of oxygen from other components can be performed as follows. By cooling down the reaction mixture, first, sulfuric acid is condensed and separated. The residual gaseous mixture composed mainly of sulfur dioxide, oxygen, and water are directly fed to the Bunsen reactor where sulfur dioxide and water are absorbed and separated from oxygen.

#### 4. Process Flowsheeting

Since the thermochemical process is a kind of energy conversion process, the efficiency of energy conversion is an important factor. The efficiency is usually defined as the ratio of Higher Heating Value (HHV) of hydrogen to the net external heat input to the process, and is called "thermal efficiency".

Preliminary flowsheet of the process has been studied, in accordance with the progress of the study on the process chemistry, to evaluate the possible thermal efficiency and to make clear the research field for improving the process. In the flowsheeting studies, the efforts were made to minimize the net external heat such as to use internal heat exchanging system.

The basic flowsheet of the process can be drawn as shown in Fig.4.1 based on the knowledge of the chemistry of the reactions and separations. Here, there are two or three candidates concerning the processing of the  $\text{HI}_x$  solution (distillation and decomposition) as described in chapter 3.

In the early 80's, GA published a flowsheet[18]. The representative process conditions and the temperature range of He from HTGR adopted in the flowsheeting were as follows.

(a) Bunsen reaction step

Bunsen reaction:  $>386.5\text{K}$ ,

Phase separation:  $368\text{K}$

(b) HI decomposition step

Distillation: Extractive distillation utilizing  $\text{H}_3\text{PO}_4$ . The diluted phosphoric acid is concentrated by multi-stage vapor recompression evaporation

HI Decomposition: Liquid phase decomposition with homogeneous catalyst(Pd) at  $393\text{K}$ ,  $5.06\text{MPa}$ . conversion of HI is ca. 52%.

Product separation: Distillation for  $\text{HI}-\text{I}_2$  separation, and cooling for  $\text{HI}-\text{H}_2$  separation. HI is sent back to the decomposer, and  $\text{I}_2$  is returned to the Bunsen reactor.

(c) Sulfuric acid decomposition step

Concentration & Vaporization: Multi-stage flash evaporation at  $202\text{kPa}$ .

Decomposition: At  $1143\text{K}$ ,  $202\text{kPa}$  with  $\text{Fe}_2\text{O}_3$  catalyst.

Product Separation: Cooling for undecomposed  $\text{H}_2\text{SO}_4$  separation, other components are directly fed to the Bunsen reactor where  $\text{O}_2$  is separated.

(d) Utilization temperature range of Helium from HTGR



773K – 1263K

In the flowsheet, internal heat exchange considering thermal match-up was included as much as possible. Also, low temperature heat was recovered by freon cycle power generation systems, and the recovered power was used in the process. With the flowsheet, thermal efficiency of 47% was estimated.

Researchers of RWTH proposed modifications of the GA flowsheet in two fields. One concerned the sulfuric acid decomposition step, where multiple effect evaporators were introduced instead of the multi-stage flash evaporator[38]. It was estimated that with the modification the exergy loss in the sulfuric acid decomposition step reduced ca. 25%. Another modification concerned the hydrogen iodide decomposition step, where the reactive distillation method was introduced instead of the extractive distillation using phosphoric acid[39]. With these modifications, the process thermal efficiency was estimated to be improved to >50%.

Recently, Prof. Bilgen's group at University of Montreal published a new concept on the flowsheet of the sulfuric acid decomposition step[40]. In the flowsheet, oxygen gas was used as a heat carrier which absorbed the nuclear heat from helium at gas-gas heat exchangers. The sensible heat of the oxygen was used to concentrate and vaporize the sulfuric acid by direct contact in adiabatic reactors. The method avoids the critical problems of the selection of structural materials for the sulfuric acid vaporizer where the process environment is very corrosive. The cost of processing a unit amount of  $\text{SO}_2$  was estimated, considering the costs of structural materials and nuclear heat, and compared with the method of GA and that of RWTH. It was concluded the cost of the method lied between that of RWTH and that of GA.

These studies revealed that a thermal efficiency higher than 40% is attainable, and the efficiency was found to depend strongly on the conversion ratio of HI, the HI/ $\text{H}_2\text{O}$  ratio of the distillate from the HIx distillation column, and the efficiency of heat recovery.

## 5. Structural Materials

A special consideration is required on the structural materials for the process, because the process fluid constitutes very corrosive environments. Since sulfuric acid and halogen compounds are widely used as the circulating chemicals in many thermochemical processes, the selection of corrosion resistant materials for plant construction has been performed in many research institutions. In the followings, the results of the corrosion tests of commercially available materials carried out at Chiyoda Corporation entrusted by JAERI are summarized. The related knowledge reported from other research institutions is also included.

The tests were performed for some representative process environments using test pieces of the size of 10mm x 40mm x 3-5mm. The process environments were simulated in quartz glass flasks in the case of static and boiling liquid conditions, and in flow reactors made of quartz tube in the case of vapor conditions. The test pieces, whose surfaces were smoothened with #600 sand paper before the tests, were exposed to the simulated environments for specified duration. After exposure, the changes of weight and appearance were observed.

### 5.1 Bunsen Reaction Step

Environment:

- a) 50% $\text{H}_2\text{SO}_4$ +0.1% $\text{HI}$ , Liquid, 393K, 101kPa.
- b)  $\text{HI}_x$ +0.1% $\text{H}_2\text{SO}_4$ , Liquid, 393K, 101kPa.

Duration of exposure: 100hr, 1000hr.

Materials tested:

- a) High Si cast iron (15%Si), Hastelloy C-276, Pb, Ta, Zr, Teflon PFA (PerFluoroAlkylvinylether), PPS(PolyPhenylene Sulfide),  $\text{SiO}_2$ , SiC,  $\text{Si}_3\text{N}_4$ .
- b) High Si cast iron (15%Si), Hastelloy C-276, Ta, Zr, Ti, Teflon PFA,  $\text{SiO}_2$ , SiC,  $\text{Si}_3\text{N}_4$ .

Results(see Fig. 5.1):

Hastelloy C-276 was corroded severely in the both environments. High Si cast iron was corroded a little in the environment a), however, corroded severely in the environment b). Ti showed relatively good corrosion resistance in the environment b), the corrosion rate of which was 0.17mm/y. Other metals, i.e., Ta, Zr and Pb, showed excellent corrosion resistance in the testing environments, the corrosion rate of which were lower than 0.05mm/y. Polymers, PFA and PPS, showed a little weight increase, and in

the environment b) the color of surfaces changed. Ceramics themselves showed excellent corrosion resistance, however, slight dissolution of the binder materials was observed.

Concerning the environment of  $\text{HI}_x$  solution ( $\text{HI}/\text{I}_2/\text{H}_2\text{O}=11/82/7$  in wt%) at 398K, GA performed a corrosion test[41]. With 500hr exposure tests, Ta and Nb were found to be resistant to the environment. Mo also showed relatively good corrosion resistance although grain boundary attack was observed. In contrast to our results at 393K, Zr was reported to be corroded severely at 398K.

## 5.2 Hydrogen Iodide Decomposition Step

### 5.2.1 Distillation

Environment:

a)  $\text{HI}_x$  ( $\text{HI}/\text{I}_2/\text{H}_2\text{O}=1/94/5$  in mol), Liquid, 573K, 2.02MPa.

b)  $\text{HI}_x$  ( $\text{HI}/\text{I}_2/\text{H}_2\text{O}=13/5/82$  in mol), Liquid, 513K, 2.02MPa.

Duration of exposure: 20hr, 100hr.

Materials tested:

SUS316, Incoloy 825, Hastelloy C-276, SN-3, Ta, Zr, Nb, Ti, SiC,  $\text{ZrO}_2$ .

Results(see Fig. 5.2):

Ta and SiC showed excellent corrosion resistance in the both environments. Nb showed no weight change in the environment a), however, was corroded a little, 0.4mm/y, in the environment b). On the contrary, Zr showed no weight change in the environment b), while was corroded, 0.5mm/y, in the environment a).  $\text{ZrO}_2$  showed excellent corrosion resistance in the environment a), however, was decomposed in the environment b). Other metals showed no corrosion resistance.

The environments of the tests concern the reactive distillation column conditions proposed by RWTH. Although Ta showed excellent result as described above, it should further be considered that hydrogen is produced at the top of the column in the reactive distillation. On the extractive distillation using phosphoric acid proposed by GA, no information is available at present on the suitable structural materials for the column.

### 5.2.2 Decomposition Reaction

Environment:

a) 57wt%HI, boiling condition, 101kPa.

- b)  $\text{HI}_x$  ( $\text{HI}/\text{I}_2/\text{H}_2\text{O}=1/1/6$  in mol), Vapor, 473K, 101kPa.
- c)  $\text{HI}_x$  ( $\text{HI}/\text{I}_2/\text{H}_2\text{O}=1/1/6$  in mol), Vapor, 573K, 101kPa.
- d)  $\text{HI}_x$  ( $\text{HI}/\text{I}_2/\text{H}_2\text{O}=1/1/6$  in mol), Vapor, 673K, 101kPa.

Duration of exposure:

- a) 20hr, 100hr.
- b)-d) 96h, 1000h.

Materials tested:

- a) SUS316, Incoloy 825, Hastelloy C-276, SN3, Ta, Zr, Nb, Ti, SiC,  $\text{ZrO}_2$ .
- b)-d) SB42, SCMV3, SUS405, SUS444, SUSXM27, SUS304, SUS316L, SUS310S, SUS329J1, Incoloy 800, Incoloy 825, Inconel 600, Hastelloy C-276, Ta, Zr, Ti, SiC,  $\text{Si}_3\text{N}_4$ .

Results(see Fig. 5.3):

In the boiling condition a), Ta, Zr, Nb, SiC, and  $\text{ZrO}_2$  showed excellent corrosion resistance, the corrosion rate of which were lower than 0.1mm/y. Hastelloy C-276 also showed relatively good corrosion resistance, ca. 0.2mm/y. Other metals showed no corrosion resistance.

In the short term exposure to the gas phase conditions at 473K, Ti, Ta, Zr, SiC,  $\text{Si}_3\text{N}_4$ , Inconel 600, and Hastelloy C-276 showed excellent corrosion resistance. Other metals suffered a little corrosion, 0.1-1.2 mm/y. The effect of temperature increase from 473K to 673K was little. The long term exposure tests were carried out with SCMV3, SUS444, SUS316L, Hastelloy C-276, Inconel 600, and Ti. In the long term exposure, Ti, Hastelloy C-276, and Inconel 600 showed excellent corrosion resistance at the temperature range studied. The other metals suffered a little corrosion, ca. 0.1 mm/y.

The studied gas phase conditions refer to the upstream environment of the decomposition reactor where hydrogen is not present. The corrosion tests of metals in the presence of hydrogen were performed at NCL[42] using a thermobalance. It is reported that, under the atmosphere of  $\text{HI}/\text{I}_2/\text{H}_2\text{O}/\text{H}_2=10.3/5.2/55.2/29.2$  (in molar ratio) at 473-723K, hydrogen absorption was observed with Hastelloy C, Ti, and Ta. Mo was reported to show an excellent result. They also reported the results on non-metallic materials that the oxide materials(alumina, mullite etc.) and graphite showed a good corrosion resistance at 773K and 973K[43]. Pyroceram type glass lining was reported to be compatible at 473K and 773K.

Referring to the liquid phase HI decomposition reactor, GA conducted corro-

sion tests for a dry HI-I<sub>2</sub> mixture environment using a glass autoclave and a bench scale unit for the HI decomposition[41]. Hastelloy B-2, which showed excellent corrosion resistance at 323K and 1.11MPa, was reported to be corroded at engineeringly interested temperature and pressure of 403K and 3.34MPa.

### 5.3 Sulfuric Acid Decomposition Step[44]

#### 5.3.1 Concentration and Vaporization

Environment:

- a) 40wt% H<sub>2</sub>SO<sub>4</sub> with/without 1% HI+0.5% I<sub>2</sub>, boiling condition, 101kPa.
- b) 70wt% H<sub>2</sub>SO<sub>4</sub> with/without 1% HI+0.5% I<sub>2</sub>, boiling condition, 101kPa.
- c) 98wt% H<sub>2</sub>SO<sub>4</sub> with/without 1% HI+0.5% I<sub>2</sub>, boiling condition, 101kPa.

Duration of exposure: 24hr, 800hr.

Materials tested:

High Si cast iron (15%Si), SUS304, SUS316L, SUS310S, Incoloy 800, Incoloy 825, Carpenter 20Cb, 20Cr-25Ni-6Mo, Inconel 625, Inconel 600, Hastelloy B-2, Hastelloy C-276, Hastelloy G-3, Monel 400, Ta, Zr, Pb.

Results(see Fig. 5.4):

In the boiling condition of 40wt% H<sub>2</sub>SO<sub>4</sub>, Ta and Zr showed excellent corrosion resistance irrespective of the presence of HI and I<sub>2</sub>. Pb also showed a good result. High Si cast iron, Hastelloy B-2, and Monel 400 were good in pure sulfuric acid, but corroded in the presence of HI and I<sub>2</sub>. Other metals had no resistance to the environment.

The results in the boiling 70wt% H<sub>2</sub>SO<sub>4</sub> were similar to that in the 40 wt% H<sub>2</sub>SO<sub>4</sub> except those of Pb, Hastelloy B-2, and Monel 400 which had no resistance in the concentrated solution.

On the contrary, in the boiling condition of 98wt% H<sub>2</sub>SO<sub>4</sub>, only High Si cast iron showed excellent corrosion resistance irrespective of the presence of HI and I<sub>2</sub>. Ta was decomposed in the environment.

The corrosion resistance for 98wt% H<sub>2</sub>SO<sub>4</sub> in the absence of HI nor I<sub>2</sub> at higher temperature and pressure was tested at WH using quartz capsules set in an pressurized stainless steel vessel[45]. Tests were carried out at up to 725K and 2.02MPa for 1000h. Silicon, CVD SiC, and hot pressed Si<sub>3</sub>N<sub>4</sub> were found to have good corrosion resistance. The researchers of WH selected SiC be an promising candidate, considering not only the corrosion resistance but also an ongoing project on the ceramic heat exchangers using SiC for coal gasification.

The researchers of JRC Ispra proposed a process where no metallic heat exchanger was needed[46]. In the process, the sulfuric acid is concentrated and vaporized by direct contact with hot air in an adiabatic reactor with refractory bricks and metallic pressure vessel. The refractory bricks works as an anti-corrosive layer and also as an insulator to protect metallic vessel. The process was called "CRISTINA", and the concept has been improved by Bilgen et al. as described in chapter 4.

### 5.3.2 Decomposition Reaction

#### Environment:

- a)  $\text{H}_2\text{O}+\text{SO}_3$  gaseous mixture obtained by vaporizing 98wt% $\text{H}_2\text{SO}_4$ , 1073K, 1123K, 1173K, 101kPa.
- b)  $\text{H}_2\text{O}+\text{SO}_2+\text{SO}_3+\text{O}_2$  gaseous mixture obtained by the contact of mixture a) with  $\text{Fe}_2\text{O}_3$  catalyst, 1073K, 1123K, 1173K, 101kPa.

Duration of exposure: 50hr(1073K & 1173K), 1000hr(1123K).

#### Materials tested:

SUS304, SUS310S, SUS316L, SUS329J1, SUS405, Incoloy 800, Incoloy 825, Inconel 625, Inconel 600, Hastelloy B-2, Hastelloy G-3, Hastelloy C-276, Hastelloy XR, IN657, IN690, SSS113MA, NSC1, SZ, Zr.

#### Results(see Fig. 5.5):

There was no large difference in the corrosion resistance of the metals tested except Hastelloy B-2, Zr, and SUS405 which showed poor resistance to the environments. The surfaces of most of the test pieces examined were covered with thin compact scales, and the corrosions were found to occur along the grain boundary. The environment a) was found to be more aggressive than the environment b).

In the short term exposure at 1173K, the corrosion depths of the metals except Hastelloy B-2, Zr, and SUS405 were between 40 $\mu\text{m}$  to 100 $\mu\text{m}$  in the environment a), whereas between 8 $\mu\text{m}$  to 40 $\mu\text{m}$  in the environment b). In the long term exposure at 1123K, those were between 90 $\mu\text{m}$  to 200 $\mu\text{m}$  in the environment a), and 10 $\mu\text{m}$  to 100 $\mu\text{m}$  in the environment b).

The environments were examined also at WH[45], JRC Ispra[47], and GA[48]. Especially, at JRC Ispra and at GA, metallic reactors were fabricated and demonstrated though the service duration were quite limited in both cases. In the both cases, Incoloy 800 was selected as the reactor material by corrosion tests in laboratory. The decomposers constructed had size corresponded to 30-40kg/h. At JRC, Ispra, it was operated in a dry  $\text{SO}_3/\text{SO}_2$  circulation at 1153K for 122hr.

## 6. Laboratory Scale Demonstration

In parallel with the above mentioned studies, process demonstration has been attempted in laboratory scale at GA and at JAERI.

The first demonstration was done at GA[18]. The apparatus, which was called "Closed-Loop Cycle Demonstrator (CLCD)", was made of glass and quartz, and composed of Bunsen reactor,  $\text{HI}_x$  purifier, HI decomposer,  $\text{H}_2\text{SO}_4$  purifier, and  $\text{H}_2\text{SO}_4$  decomposer. The distillation of  $\text{HI}_x$  was not included. The apparatus was operated subsequently in a recycle mode with the hydrogen production rate of 1.2 l/hr.

Following the CLCD, GA built an apparatus which aimed at the study of continuous operation condition of the scheme adopted in their flowsheet[18]. It was designed to be the size of 60 l- $\text{H}_2$ /hr, and made of mainly glass and quartz. The following achievements were reported with the apparatus operated at atmospheric pressure.

- a) The Bunsen reaction could be carried out at designed condition.
- b) The purification of the sulfuric acid phase could be performed by the counter current contact with steam.
- c) The purification, concentration, and decomposition of the sulfuric acid could be carried out simultaneously for 14 hrs.

Experiments on the HI decomposition step were reported to be unsuccessful because of the troubles of  $\text{HI}_x$  transportation, low throughput of extractive distillation column, corrosion of vessels by hot phosphoric acid, etc.

Based on the experiences reported, we have been trying to demonstrate the process in the continuous operation mode. The purpose is

- a) to show the continuous hydrogen production by IS process,
- b) to examine the possible problems caused by the recycle use of the process fluid,
- c) and to accumulate technical knowledge for designing and operating scaled up plant.

Fig.6.1 shows a simplified flow-sheet of the experimental apparatus which was designed to realize the basic functions of the process depicted in Fig.4.1. It was designed to have a capacity of 1-10 l- $\text{H}_2$ /hr, and is made of quartz, glass and teflon. Every operation is carried out under atmospheric pressure. Here, the distil-

lation of  $\text{HI}_x$  solution and the decomposition of HI have so far been carried out with conservative methods considering the simplicity of operation. Also, in order to maintain the precise rate of liquid transportation, the number of pumps which requires high precision is reduced to four, utilizing transportation by gravity as much as possible with suitable reactor arrangement.

The representative operation conditions are as follows,

(a) Bunsen reaction step

Bunsen reaction: ca.333K,

Phase separation: 283K. Iodine concentration is that of saturation at 263K.

These conditions were chosen to avoid the line plugging caused by  $\text{I}_2$  precipitation.

(b) HI decomposition step

Purification: counter-current stripping by  $\text{N}_2$  in a wetted-wall tower,

Distillation: atmospheric pressure distillation with a packed column,

HI decomposition: gas phase decomposition with  $\text{Pt/SiO}_2$ -wool catalyst at 973K with four series of reactors.

Products separation: cooling to ca.283K. Separation of hydrogen from the tail gas of each reactor by partial condensation enables to attain the once-through conversion of 50%.

(c) Sulfuric acid decomposition step

Purification & Concentration: counter-current stripping by  $\text{N}_2$  in a wetted-wall column,

Decomposition:  $\text{Pt/SiO}_2$ -wool catalyst, 1123K, conversion of  $\text{SO}_3 = 80\%$ ,

Products separation: cooling for undecomposed  $\text{H}_2\text{SO}_4$  separation, undecomposed components are directly fed to the Bunsen reactor where  $\text{O}_2$  is separated.

Preliminary experiments to confirm the performance of each reactor encountered a number of troubles, such as sulfur formation in the Bunsen reactor and  $\text{HI}_x$  distillation column, line plugging caused by iodine precipitation, and disappearance of the liquid-liquid phase separation because of the liquid transportation rate mismatch. At present, however, with modifications of the reactor design and the operation conditions, it becomes possible to operate every reactors without troubles. In the course of these studies, some useful know-how for the plant operation could also be obtained such that the density of  $\text{HI}_x$  phase is a good indicator to check the phase separation.



Based on the performance data of each reactor, the mass balance for the continuous operation was studied with the aid of equation (6). Fig.6.2 shows a possible mass flow with the present apparatus revealed by the study. Here, some modifications were done in the flowsheets to guarantee the cyclic operation.

(a) The return line from HI Decomposer was connected to the outlet of Bunsen Reactor. Also, a return line of azeotropic hydriodic acid from  $\text{HI}_x$  Distillation Column to Liquid-Liquid (LL) Separator was added. These modification aims to carry out the Bunsen reaction with absorbing solution of dilute acid concentration, and to carry out the phase separation with concentrated solution. The each condition is favorable for perfect  $\text{SO}_2$  absorption and for better separation.

(b) A direct return line of sulfuric acid phase from LL Separator to Bunsen Reactor was added which was necessary to compensate the difference of the conversions in sulfuric acid decomposition and hydrogen iodide decomposition.

So far, the joint continuous operation of the apparatus except the HI decomposer for 20hrs yielded the mass balance of HI,  $\text{H}_2\text{SO}_4$ , and  $\text{I}_2$  higher than 98%. The operation of the apparatus is underway coupling the whole steps. After completion of the present demonstration, the phase separation under higher temperature and higher iodine concentration will be tested. The innovative methods for HI decomposition step will be included in the next stage apparatus.

## 7. Future Works

With the studies described in the former chapters, it can be said that, from a scientific point of view, it was shown feasible to decompose water with the consecutive operations of the chemical reactions. Also, the process thermal efficiency higher than 40% was shown to be expected under efficient operation conditions. Concerning the structural materials suitable for the aggressive process environments, corrosion resistant materials for each process environment have been screened out by the corrosion tests for commercially available materials.

In order to improve and to realize the process, extensive studies are required. In the followings, R&D items are summarized focusing on those required for proceeding to the process demonstration coupled with HTTR. The scheme of the R&D strategy is shown in Fig. 7.1.

### 7.1 Process Chemistry & Flowsheeting

On the Bunsen reaction step, the efficient operation conditions have been almost clarified from viewpoint of the reaction and the phase equilibrium. Some additional data, e.g., the effect of hydrogen iodide concentration on the absorption of sulfur dioxide at high temperature, are required. Also, the absorption rate should be clarified in conjunction with the reactor design.

On the hydrogen iodide decomposition step, there are three possibilities for the distillation method, i.e., conventional (atmospheric pressure) distillation, extractive distillation, and reactive distillation. Also, there have been many proposals on the decomposition method, i.e., gas phase catalytic decomposition with or without iodine adsorbent, liquid phase catalytic decomposition, etc. Generally speaking, the more efficient the method is, the severer the environment for the structural materials is. In some cases, the experimental verification of the concept itself has been difficult because of the lack of corrosion resistant materials for the experimental reactor vessels. The selection of the methods will therefore be a compromise between the process efficiency and the easiness of the selection of the structural materials. Hence, studies on the flowsheeting and the corrosion resistant materials are both required. In the former study, an efficient flowsheet should be pursued by use of technologies for energy savings such as multi effect distillation. At the same time, an effort to search for a new method for the processing of the  $\text{HI}_x$  solution should be beneficial, which should be efficient from view point of thermal efficiency and should offer a mild environment for the structural materials.

New technologies such as the membrane reactor[26] and the electrolysis[49] will be considered.

On the sulfuric acid decomposition step, the basic scientific data have enough been accumulated. The engineering data acquisition for the process design will be the next target. Similar problems with that in the hydrogen iodide decomposition step exist, i.e., the corrosiveness of the process environments. Especially, the concentration and the vaporization conditions are quite aggressive. Therefore, the flowsheeting study to avoid the problem is required in conjunction with the R&D of structural materials. Prof. Bilgen's proposal is one solution to the problem. Also, since the sulfuric acid decomposition step connects the thermochemical process with HTGR, safety measures should be reflected in the flowsheeting against the possible problems such as tritium transmission, the difference of the dynamic characteristics. The considerations will be reflected to the number of reactors to be connected with the He loop, the operation pressure, etc.

## 7.2 Structural Materials

Based on the results of the corrosion tests, the following studies are required.

- a) Study on the effect of the aggressive environments on the mechanical properties of the materials selected by the corrosion tests.
- b) Study on the reactor design considering the structural integrity.

Concerning the concentrator and the boiler of sulfuric acid, and the  $\text{HI}_x$  distillation column, extensive research and development of the corrosion resistant materials may be necessary since the selected materials for the environments have more or less problems such as brittleness.

## 7.3 Process Demonstration

In order to proceed to the engineering demonstration coupled with HTTR, the following three step demonstration experiments will be required.

### a) Laboratory scale demonstration

Following the present experiments using the laboratory scale apparatus, a continuous production of hydrogen in the more efficient operation mode should be tested. In the experiments, the Bunsen reaction and the phase separation will be carried out at ca.368K with iodine concentration close to the saturation. Here, the quantitative transportation method of melted iodine

should be established. Also, an acquisition of engineering data of the purification of the acids should be carried out at this stage. Various methods for measuring and controlling the process status will be investigated.

At this stage, extensive studies on the processing of  $\text{HI}_x$  solution and on the structural materials should be carried out simultaneously to select the candidates for the next stage experiment.

#### b) Process demonstration with metallic reactors

An acquisition of the engineering data for the design of a scaled up plant is the main purpose of the experiment. At this stage, the advanced methods for hydrogen iodide decomposition step should be tested. The structural materials for the reactor vessels will be tested under the dynamic process environments. The selected methods for the measurement and control of process status will be tested. The size of the apparatus should be the minimum ones so long as the above mentioned tests can be carried out, which will be ca.  $1 \text{ m}^3\text{-H}_2/\text{hr}$ .

At this stage, an accurate process simulation and an accurate estimation of the process efficiency will be possible using the data obtained. Static and dynamic simulation of the process should be carried out under various operation conditions. Also, problems which may arise in the coupling with the heat source, HTGR, should be considered.

#### c) Scaled up process demonstration coupled with HENDEL

The final purpose of the experiments at this stage is to confirm the process characteristics under the simulated coupling condition with HTTR using large helium loop as the heat source. The sulfur trioxide decomposer and the sulfuric acid vaporizer will be the reactors to be heated by the sensible heat of helium. The key components of the heat recovery systems, which should be important from the standpoint of the process efficiency, should be tested. The long term stability of the plant operation should be demonstrated in conjunction with the establishment of the procedures for the start up, the shut down, the emergency operation etc. The size of the demonstration will be ca.  $100 \text{ m}^3\text{-H}_2/\text{hr}$ , which will be the same as that to be coupled with HTTR. With the experiments of this size, the acquisition of the process data for the commercial plant construction and for the economic evaluation will be

possible.

The process demonstration coupled with HTTR will follow the above mentioned studies. The main purpose of the experiments will be to demonstrate the long term stable and safe operation of the whole system.

### Acknowledgments

The authors express their gratitude to Mr. I. Tayama, Mr. S. Kosaka, and Mr. K. Komatsu of Chiyoda Corporation for carrying out the corrosion test of the structural materials candidates and for the useful discussions on the evaluation of the flowsheeting studies. The authors thanks to Dr. K. Hada of Department of HTTR Project, JAERI, for the useful discussions on the future works.

possible.

The process demonstration coupled with HTTR will follow the above mentioned studies. The main purpose of the experiments will be to demonstrate the long term stable and safe operation of the whole system.

### Acknowledgments

The authors express their gratitude to Mr. I. Tayama, Mr. S. Kosaka, and Mr. K. Komatsu of Chiyoda Corporation for carrying out the corrosion test of the structural materials candidates and for the useful discussions on the evaluation of the flowsheeting studies. The authors thanks to Dr. K. Hada of Department of HTTR Project, JAERI, for the useful discussions on the future works.

## References

- [1] Funk, J. and M. Reinstrom, I&EC Process Design and Develop., 5, 336-342 (1966).
- [2] EURATOM, JRC Ispra, EUR/C-IS/551/71.e(EUR4776e), 1971.
- [3] Beghi, G. E., Int. J. Hydrogen Energy, 10, 431-438(1985).
- [4] "Energy, Conversion and Utilization with High Efficiency. Subarea C, Science and Technology for Energy Conversion", ed. Y. Nishikawa and T. Matsuo, Dec. 1990.
- [5] Shimizu, S. et al., Proc. 7th Int. Conf. Emerging Nuclear Energy Systems, Makuhari, Japan, Sep. 1993, pp.532-536.
- [6] Russell, J. L. et al., Proc. 1st World Hydrogen Energy Conf., Florida, U.S.A., March 1976, p.1A-105.
- [7] Dokiya, M. et al., DENKI KAGAKU, 45, 139-143(1977).
- [8] Sato, S. et al., Proc. 3rd World Hydrogen Energy Conf., Tokyo, June 1980, vol.1, pp.389-399.
- [9] Mizuta, S. and T. Kumagai, Proc. 6th World Hydrogen Energy Conf., Vienna, July 1986, vol.2, pp.696-705.
- [10] Onuki, K. et al., Proc. 6th World Hydrogen Energy Conf., Vienna, July 1986, vol.2, pp.723-731.
- [11] Gmelins, J (1933), and Gmelins, S (1960).
- [12] Kumagai, T. et al., DENKI KAGAKU, 52, 812(1984) (in Japanese).
- [13] Shimizu, S. et al., DENKI KAGAKU, 53, 114(1985) (in Japanese).
- [14] Norman, J. H. et al., GRI-80/0105, March 1981.
- [15] Norman, J. H. et al., Proc. 2nd World Hydrogen Energy Conf., Zurich, August 1978, p.513.
- [16] Buenau, G. V. and M. Eigen, Z. Phys. Chem., 7, 108(1956).
- [17] Norman, J. H. et al., GA-A 14746, December 1977.
- [18] Norman, J. H. et al., GA-A 16713, May 1982.
- [19] Knoche, K. F. et al., Proc. 5th World Hydrogen Energy Conf., Toronto, Canada, July 1984, vol.2, p.449.
- [20] Engels, H. and K. F. Knoche, Int. J. Hydrogen Energy, 11, 703(1986).
- [21] Neuman, D., Diplom thesis, RWTH Aachen(1987).
- [22] Roth, M. and K. F. Knoche, Int. J. Hydrogen Energy, 14, 545(1989).
- [23] O'Keefe, D. R. and J. H. Norman, Proc. 3rd World Hydrogen Energy Conf., Tokyo, June 1980, vol.1, pp.277-295.
- [24] Oosawa, Y., Bull. Chem. Soc. Jpn., 54, 2908(1981).
- [25] Onuki, K. et al., Proc. 8th World Hydrogen Energy Conf., Hawaii, July 1990,

- vol.2, pp.547-556.
- [26] Ito, N. et al., Int. J. Hydrogen Energy, 9, 835(1984).
  - [27] Bodenstein, M., Z. Phys. Chem., 13, 56(1894); 22, 1(1897); 29, 295(1898).
  - [28] Trotman-Dickenson, A. F. and G. S. Milne, "Tables of Bimolecular Gas Reactions"(NSRDS-NBS9), Washington(1967).
  - [29] Oosawa, Y. et al., Nippon Kagaku Kaishi, 1980, p.1081 (in Japanese).
  - [30] Oosawa, Y. et al., Bull. Chem. Soc. Jpn., 54, 742(1981).
  - [31] O'Keefe, D. R. et al., Proc. 4th World Hydrogen Energy Conf., California, June 1982, vol.2, pp.687-701.
  - [32] Bosen, A and H. Engels, Fluid Phase Equilibria, 43, 213-230(1988).
  - [33] Sato, S. et al., JAERI-M 9724, 1981 (in Japanese).
  - [34] Ishikawa, H. et al., Proc. 3rd World Hydrogen Energy Conf., Tokyo, June 1980, vol.1, pp.297-309.
  - [35] Dokiya, M. et al., Bull. Chem. Soc. Jpn., 50, 2657(1977).
  - [36] Norman, J. H., Proc. 3rd World Hydrogen Energy Conf., Tokyo, June 1980, vol.1, pp.257-275.
  - [37] Spewock, S. et al., 1st World Hydrogen Energy Conf., Miami Beach, March 1976, p.9A-53.
  - [38] Knoche, K. F. et al., Proc. 5th World Hydrogen Energy Conf., Toronto, July 1984, vol.2, pp.487-502.
  - [39] Engels, H. and K. F. Knoche, private communication, 1986.
  - [40] Oeztuerk, I. T. et al., Trans IChemE, 72, Part A, 241-250(1994).
  - [41] Trester, P. W. and H. G. Staley, GRI-80/0081, May 1981.
  - [42] Imai, Y. et al., Corrosion Engineering (Bosyoku Gijutsu), 31, 714-721(1982) (in Japanese).
  - [43] Kondo, W. et al., Corrosion Engineering (Bosyoku Gijutsu), 31, 722-727 (1982) (in Japanese).
  - [44] Onuki, K. et al., Hydrogen Energy System(Suiso Enerugi Sisutemu), 18, 49-56(1993) (in Japanese).
  - [45] Ammon, R. L., Proc. 4th World Hydrogen Energy Conf., California, June 1982, vol.2, pp.623-644.
  - [46] Broggi, A. et al., Proc. 3rd World Hydrogen Energy Conf., Tokyo, June 1980, vol.4, pp.1929-1937.
  - [47] Coen Porisini, F., Int. J. Hydrogen Energy, 14, 267-274(1988).
  - [48] GA Technologies, GA-A17573, Feb. 1985.
  - [49] Struck, B. D. et al., Int. J. Hydrogen Energy, 5, 487-497(1980).



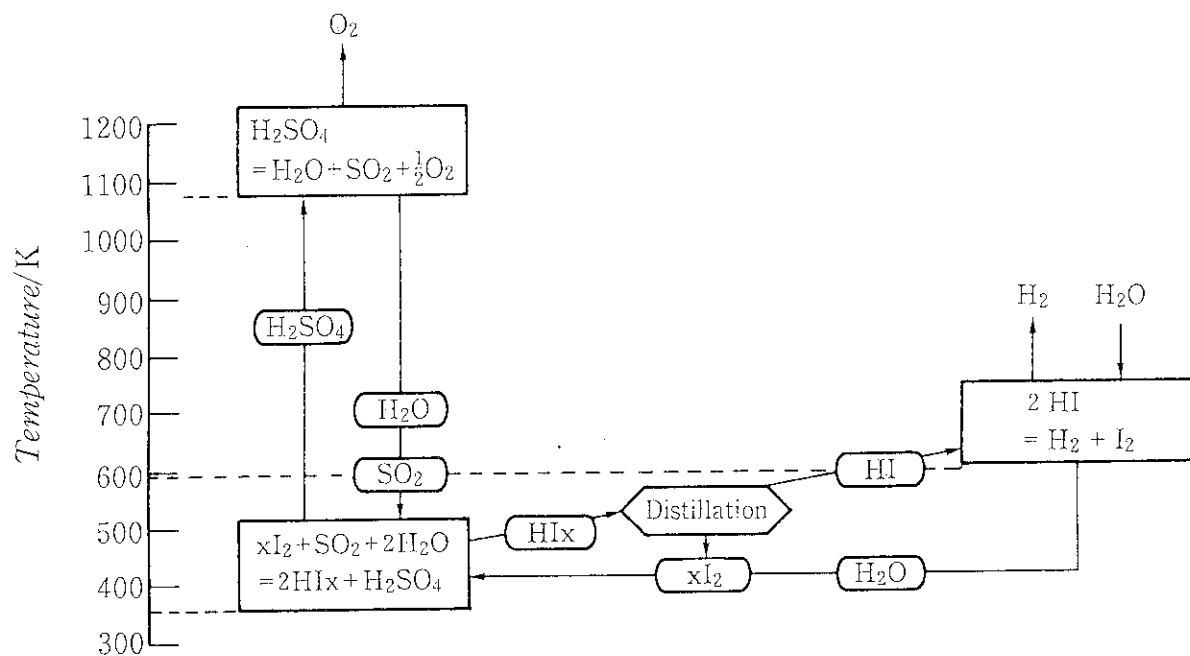


Fig. 2.1 Reaction scheme of the IS process featuring liquid-liquid phase separation of HI and  $\text{H}_2\text{SO}_4$ .

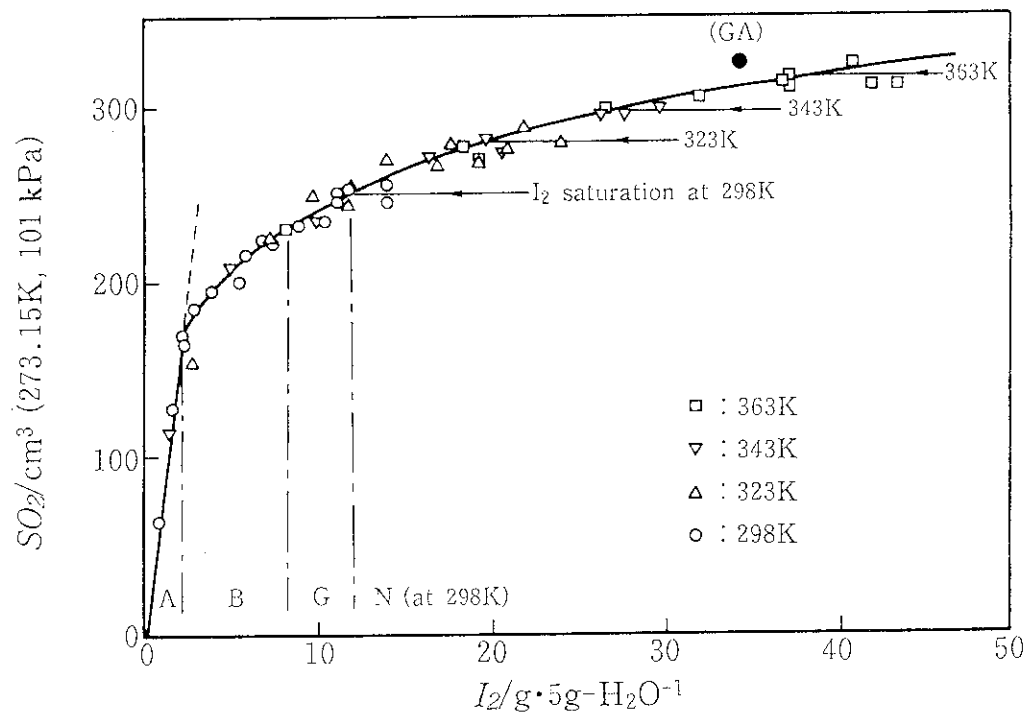


Fig. 3.1 Absorption limit of  $\text{SO}_2$  by the Bunsen reaction vs. the initial iodine fraction in the absorbent.

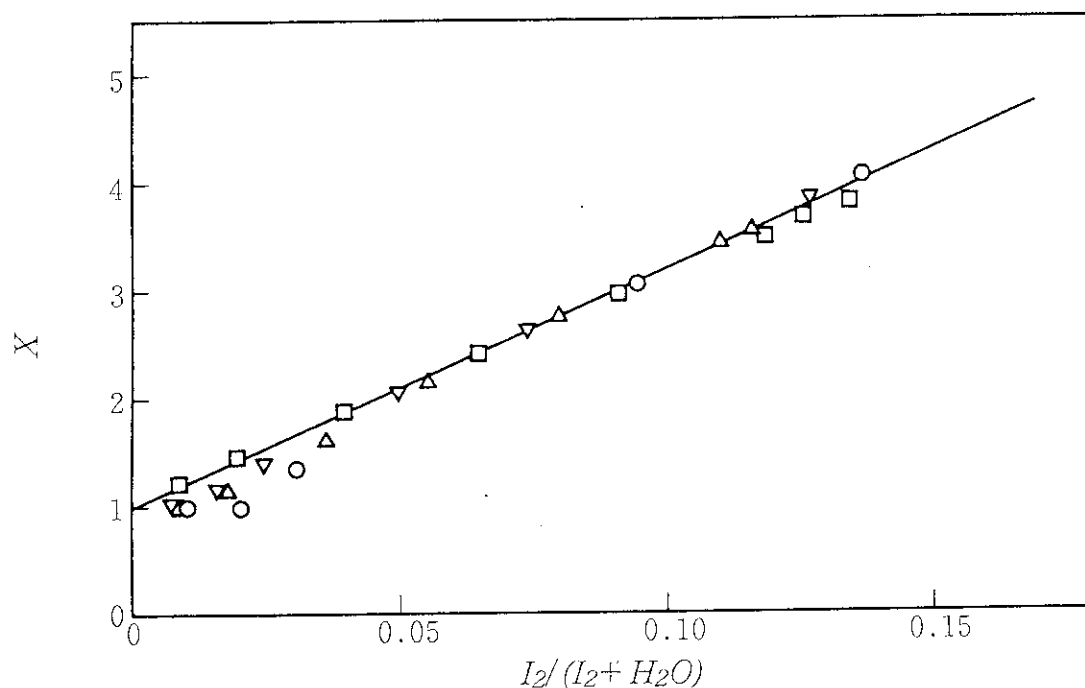


Fig. 3.2 Effect of initial HI concentration on the absorption limit of  $\text{SO}_2$  by the Bunsen reaction at 298K.

"X" denotes the ratio of the number of total iodine atoms to that of iodide ions in the product solution.

" $\text{I}_2/(\text{I}_2+\text{H}_2\text{O})$ " denotes the initial mole fraction of iodine.

Initial molar ratio of  $\text{HI}/(\text{HI}+\text{H}_2\text{O})$ ;  $\circ$  : 0.00,  $\triangle$  : 0.02,  $\nabla$  : 0.04,

$\square$  : 0.07.

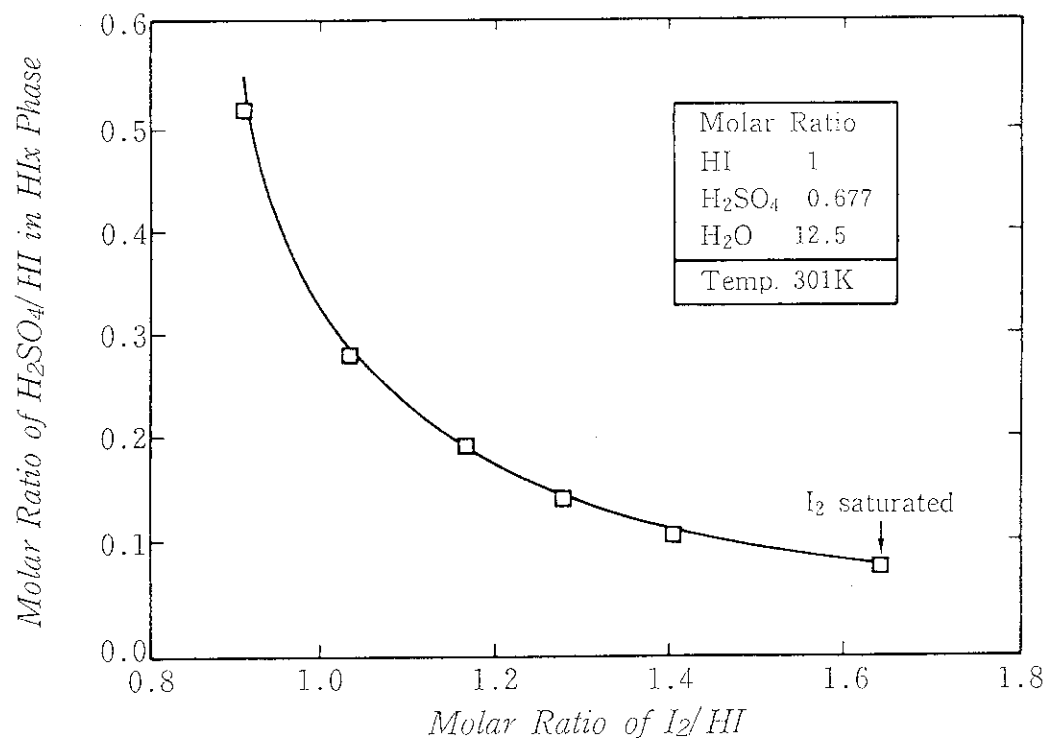


Fig. 3.3 Effect of iodine concentration on the phase separation.

"Molar Ratio of  $\text{I}_2/\text{HI}$ " denotes the molar ratio in the mixture.

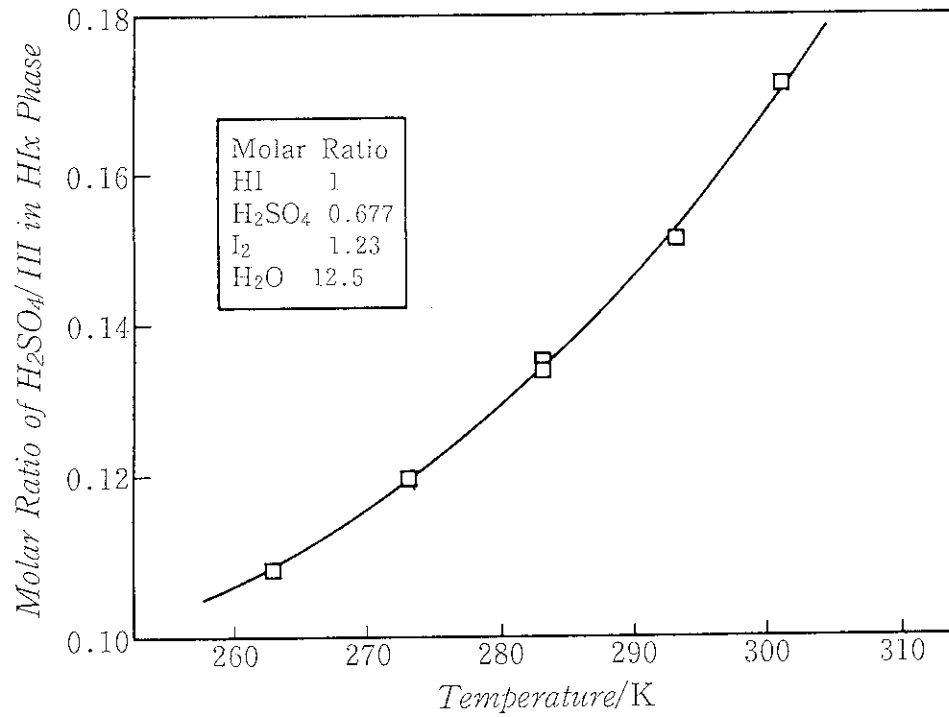


Fig. 3.4 Effect of temperature on the phase separation.

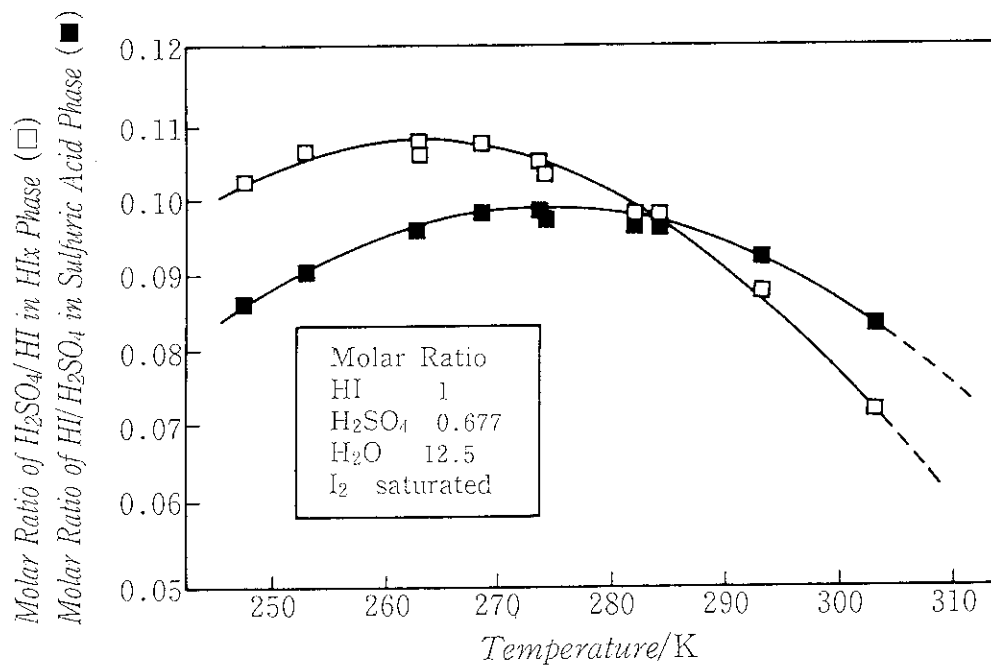


Fig. 3.5 Effect of temperature on the phase separation under iodine saturation.

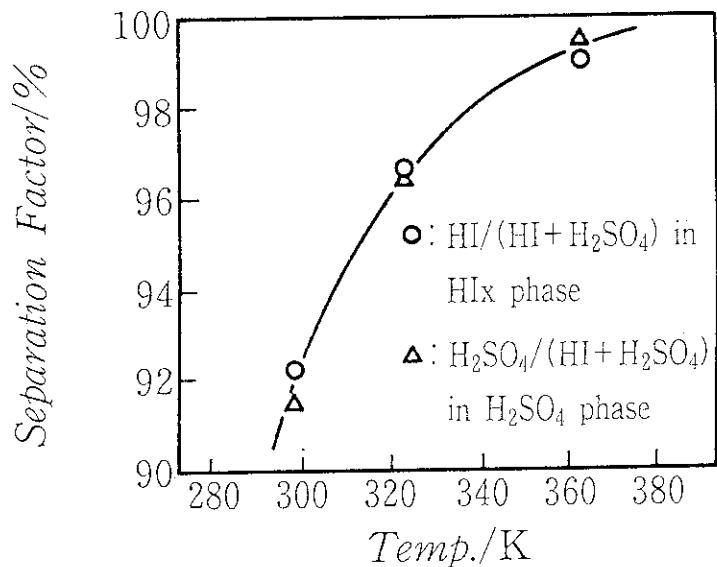


Fig. 3.6 Effect of temperature on the separation factor of the product solution obtained by the Bunsen reaction under iodine saturation.  
The "separation factor" is defined as a molar ratio shown in the figure.

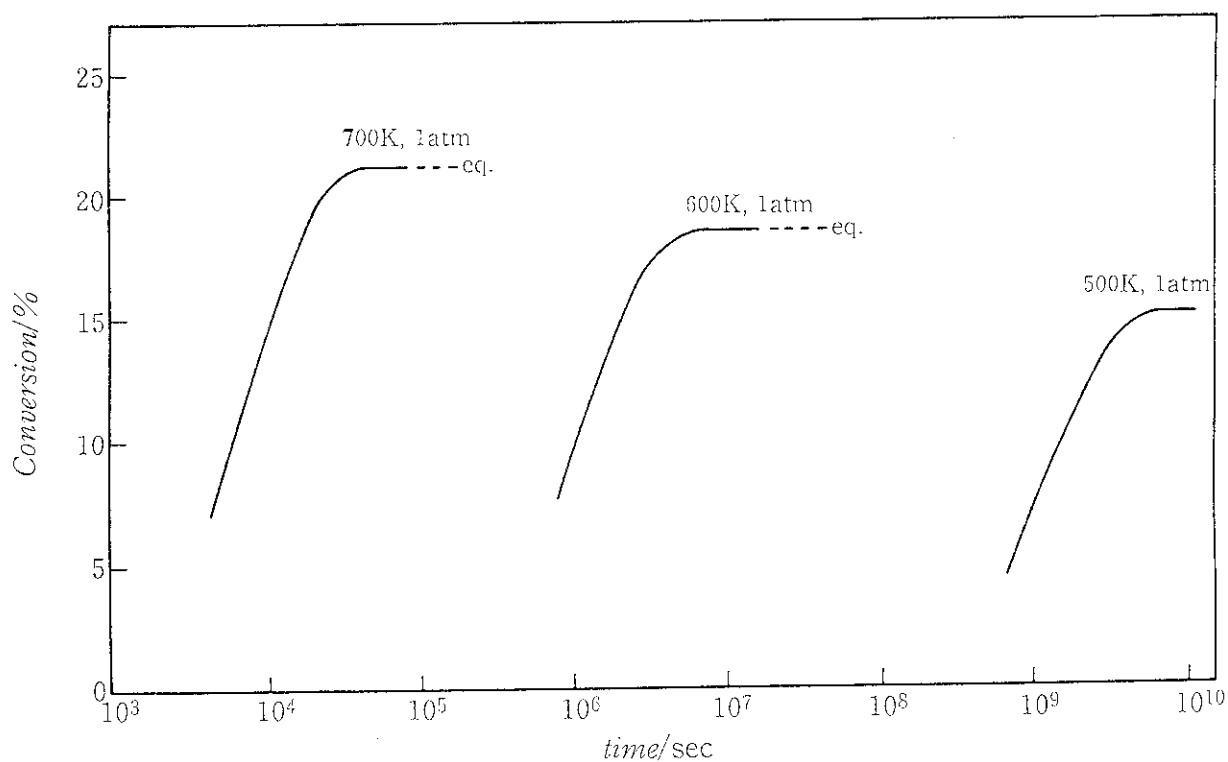


Fig. 3.7 Conversion vs. time of the homogeneous gas phase decomposition of HI.

"eq." means the equilibrium conversion ratio at the temperature.

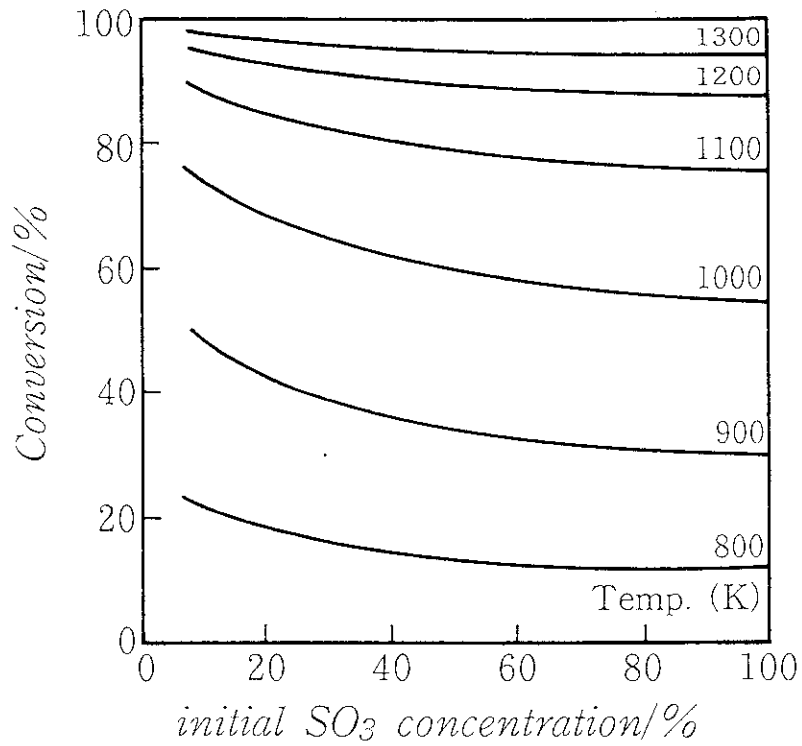


Fig. 3. 8 Effect of initial  $\text{SO}_3$  concentration on equilibrium conversion of  $\text{SO}_3$  at 1 atmospheric pressure[33].

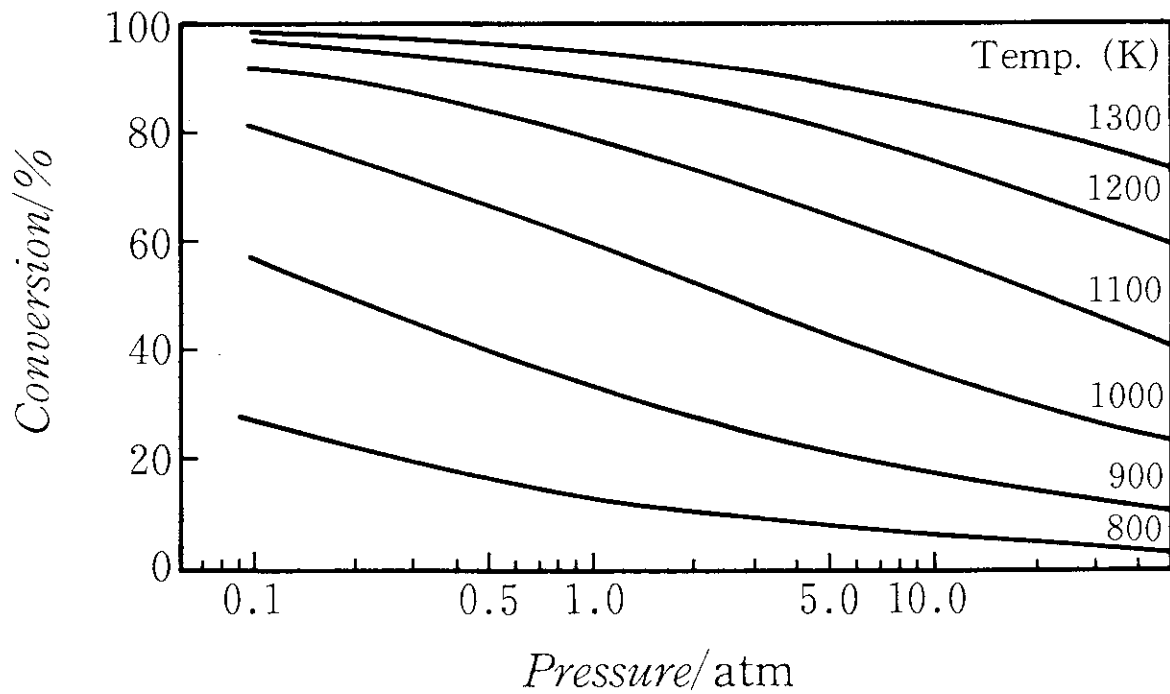


Fig. 3. 9 Effect of pressure on equilibrium conversion of  $\text{SO}_3$ .  
Initial concentration of  $\text{SO}_3$  is 100%[33].

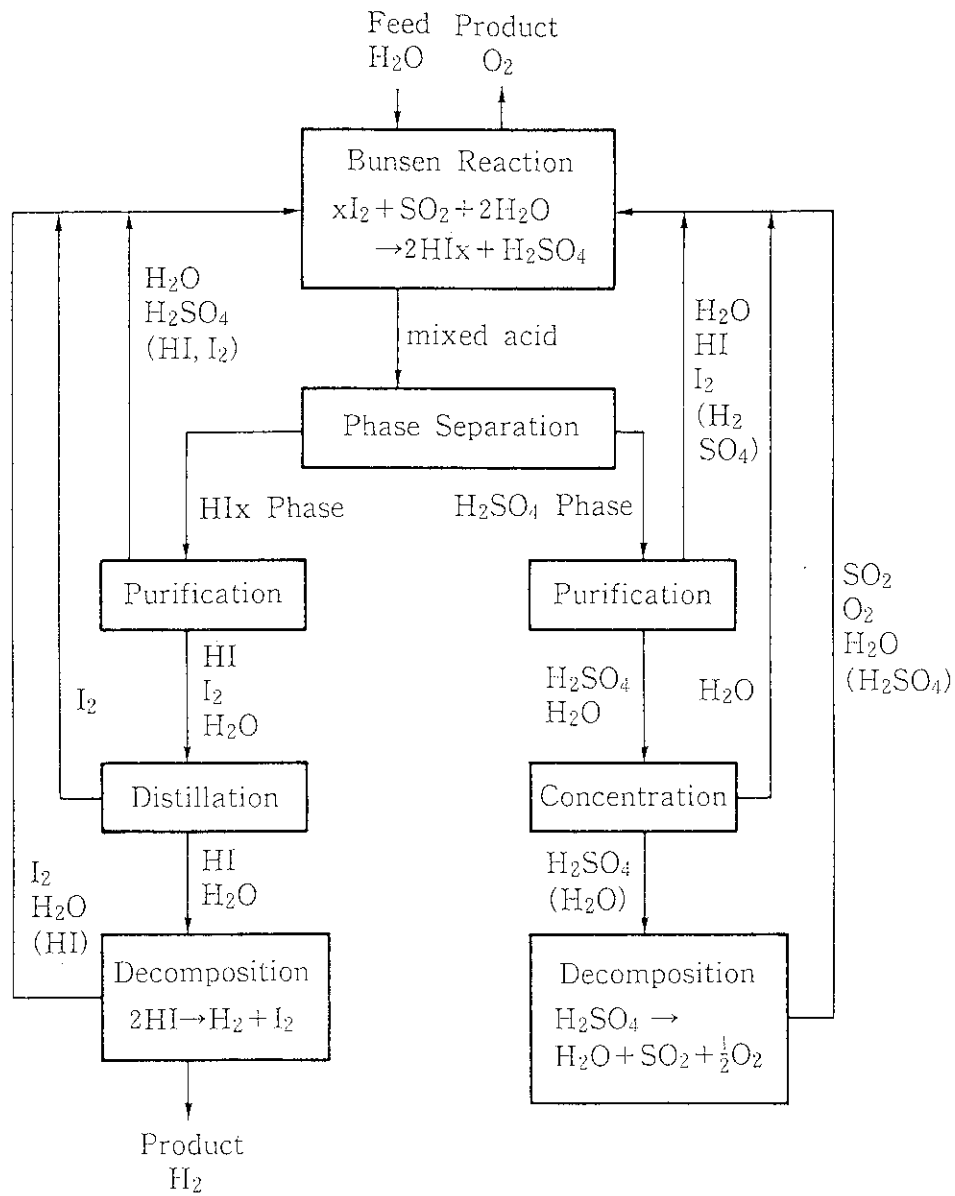


Fig. 4.1 Schematic flow diagram of IS process.

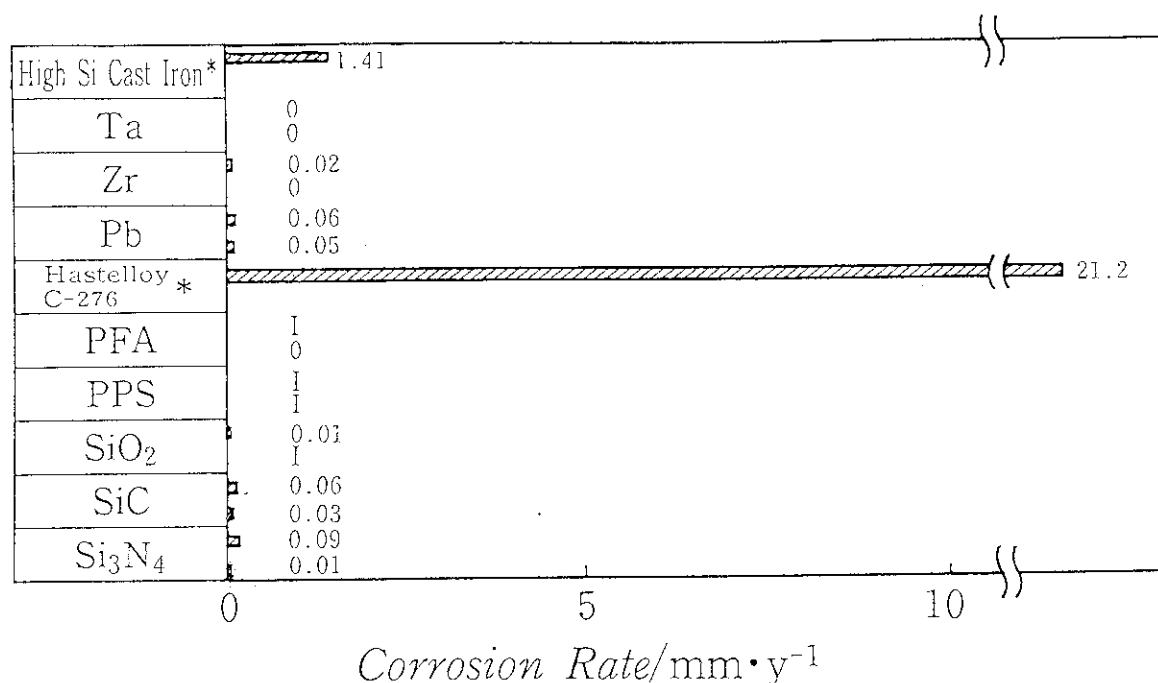


Fig. 5. 1(a) Corrosion rates in the simulated sulfuric acid phase solution (50wt% H<sub>2</sub>SO<sub>4</sub>+0.1wt% HI) at 393K.

Duration of exposure: 100hr(upper line), 1000hr(lower line).

"I" means the weight increase.

\*) Only short term exposure test was carried out.

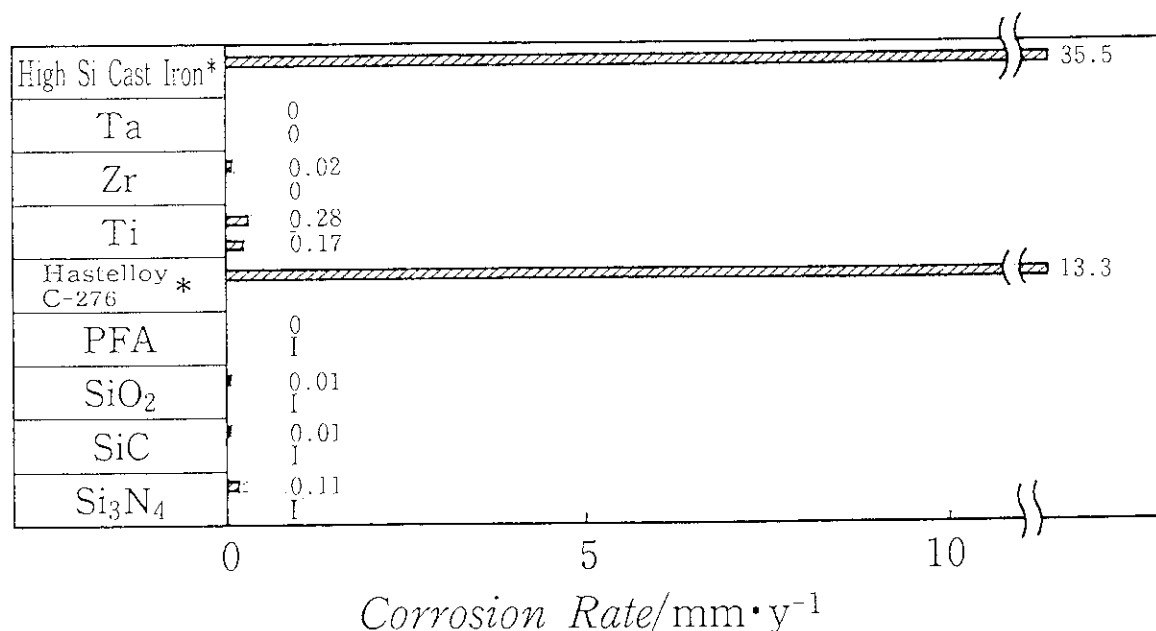


Fig. 5. 1(b) Corrosion rates in the simulated HI<sub>x</sub> phase solution

(HI<sub>x</sub>(molar ratio of HI/I<sub>2</sub>/H<sub>2</sub>O=1/1/6)+0.1wt% H<sub>2</sub>SO<sub>4</sub>) at 393K.

Duration of exposure: 100hr(upper line), 1000hr(lower line).

"I" means the weight increase.

\*) Only short term exposure test was carried out.

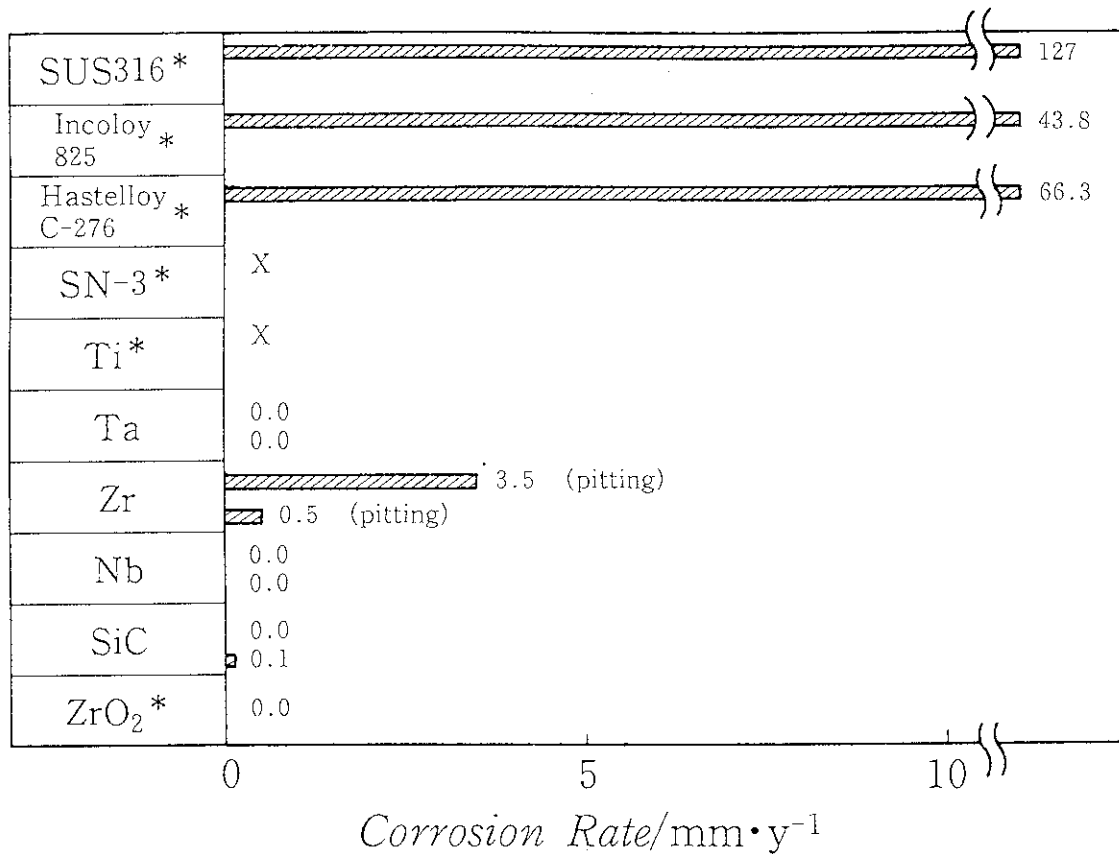


Fig. 5. 2(a) Corrosion rates in the simulated HI<sub>x</sub> distillation column environment.

HI<sub>x</sub>(molar ratio of HI/I<sub>2</sub>/H<sub>2</sub>O=1/94/5) soln. at 573K and 2.02MPa.

Duration of exposure: 20hr(upper line), 100hr(lower line).

"X" means the test piece was dissolved.

\*) Only short term exposure test was carried out.



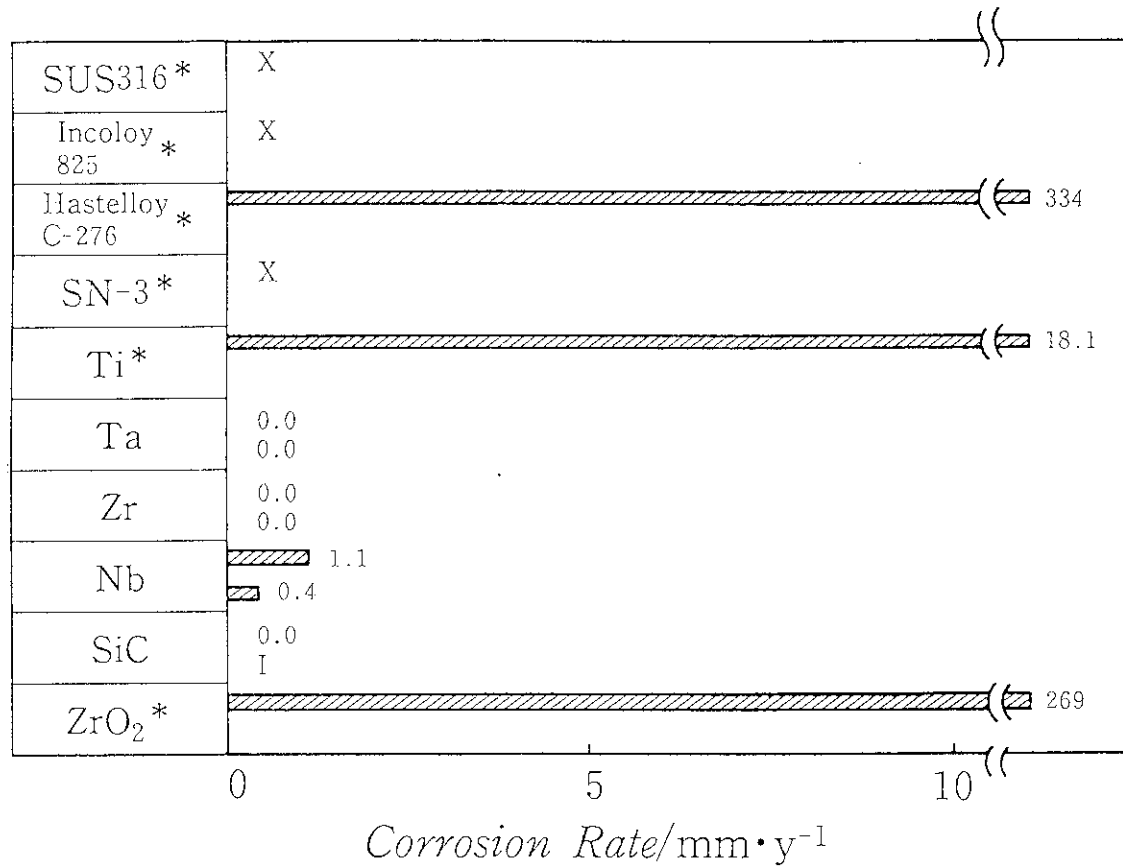


Fig. 5. 2(b) Corrosion rates in the simulated HI<sub>x</sub> distillation column environment.

HI<sub>x</sub>(molar ratio of HI/I<sub>2</sub>/H<sub>2</sub>O=13/5/82) soln. at 513K and 2.02MPa.

Duration of exposure: 20hr(upper line), 100hr(lower line).

"I" means the weight increase.

"X" means the test piece was dissolved.

\*) Only short term exposure test was carried out.

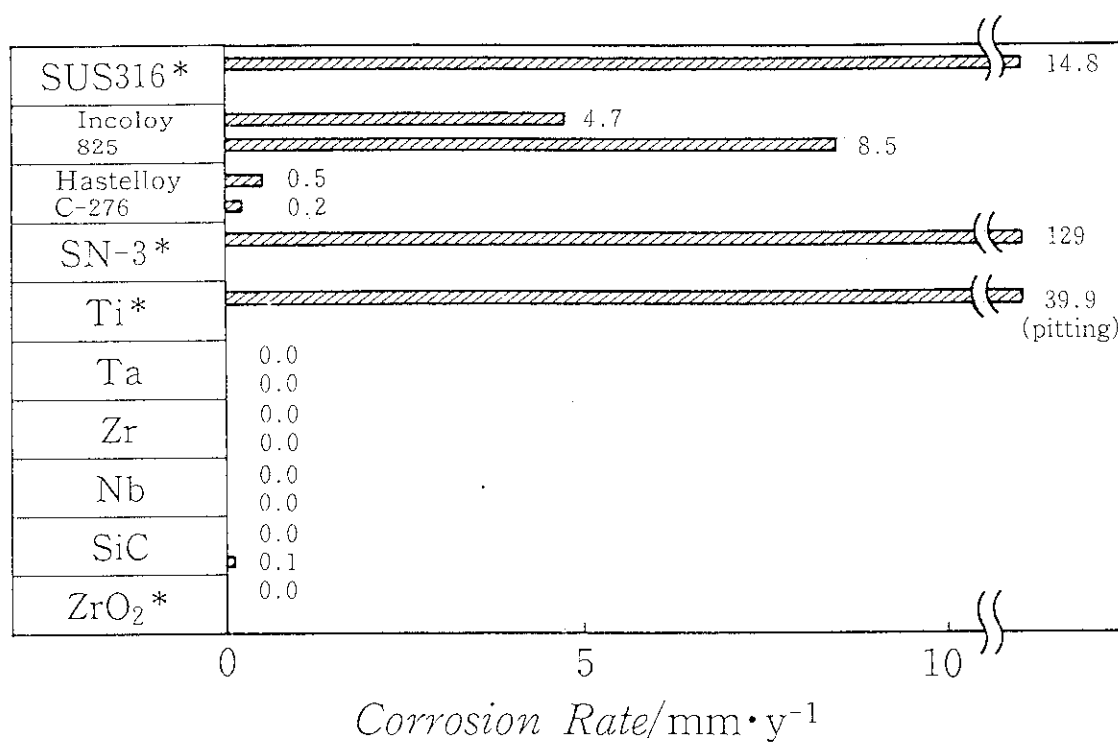


Fig. 5.3(a) Corrosion rates in the simulated HI vaporizer environment.

Boiling 57wt% HI soln. (ca. 400K).

Duration of exposure: 20hr(upper line), 100hr(lower line).

\*) Only short term exposure test was carried out.

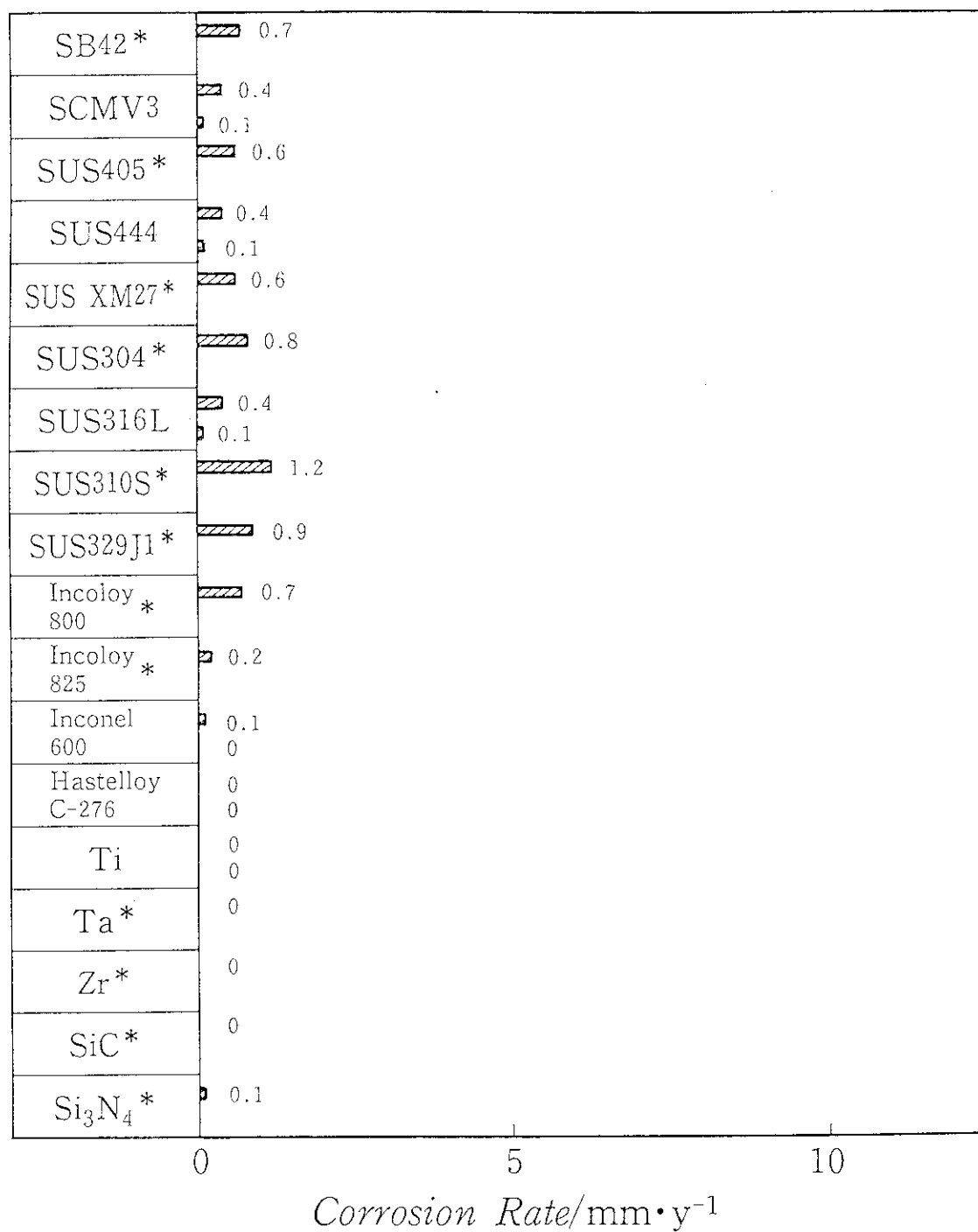


Fig. 5. 3(b) Corrosion rates in the simulated gaseous HI decomposer environment.

Molar ratio of HI/I<sub>2</sub>/H<sub>2</sub>O=1/1/6 at 473K.

Duration of exposure : 96hr(upper line), 1000hr(lower line).

\*) Only short term exposure test was carried out.

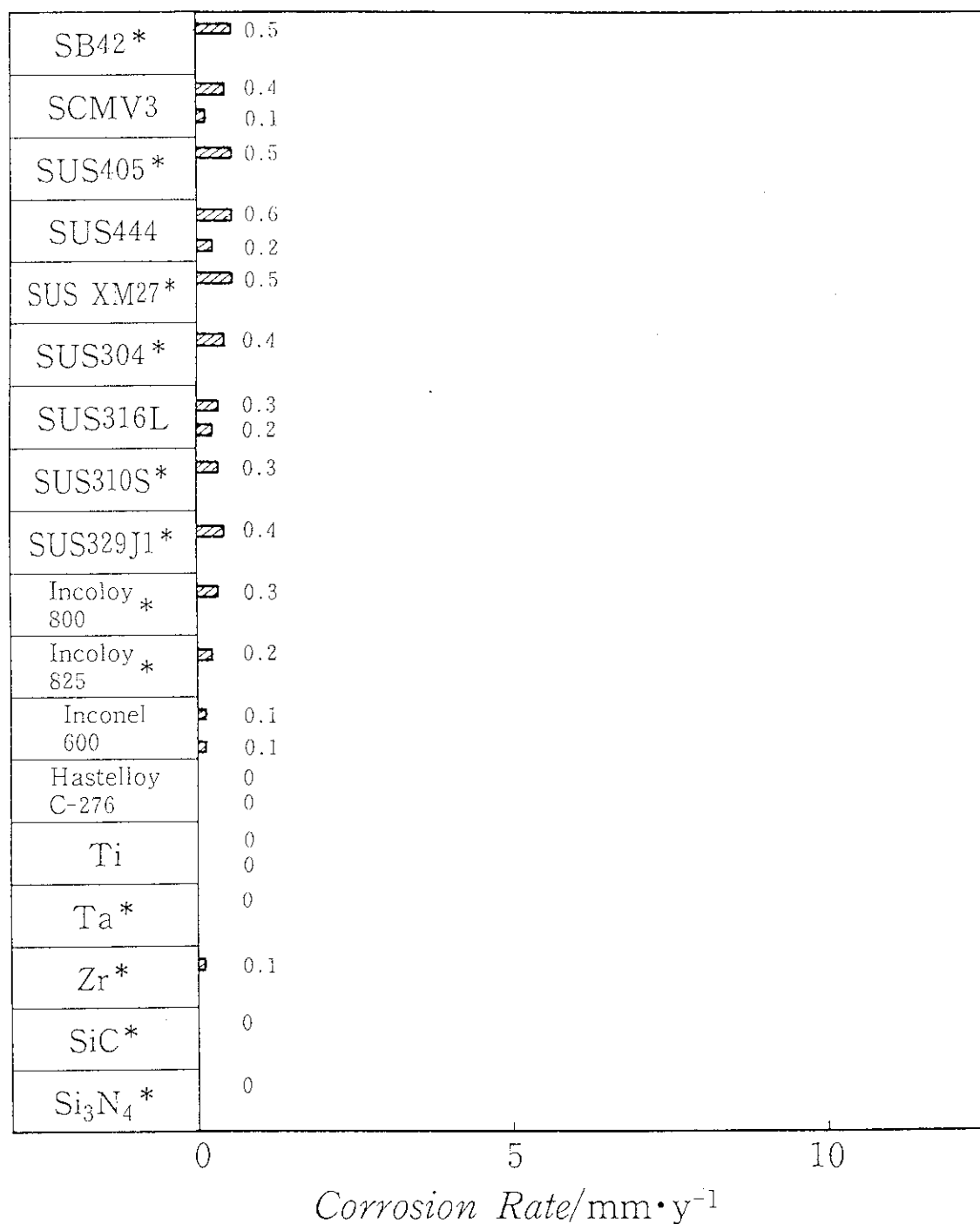


Fig. 5. 3(c) Corrosion rates in the simulated gaseous HI decomposer environment.

Molar ratio of HI/I<sub>2</sub>/H<sub>2</sub>O=1/1/6 at 573K.

Duration of exposure: 96hr(upper line), 1000hr(lower line).

\*) Only short term exposure test was carried out.

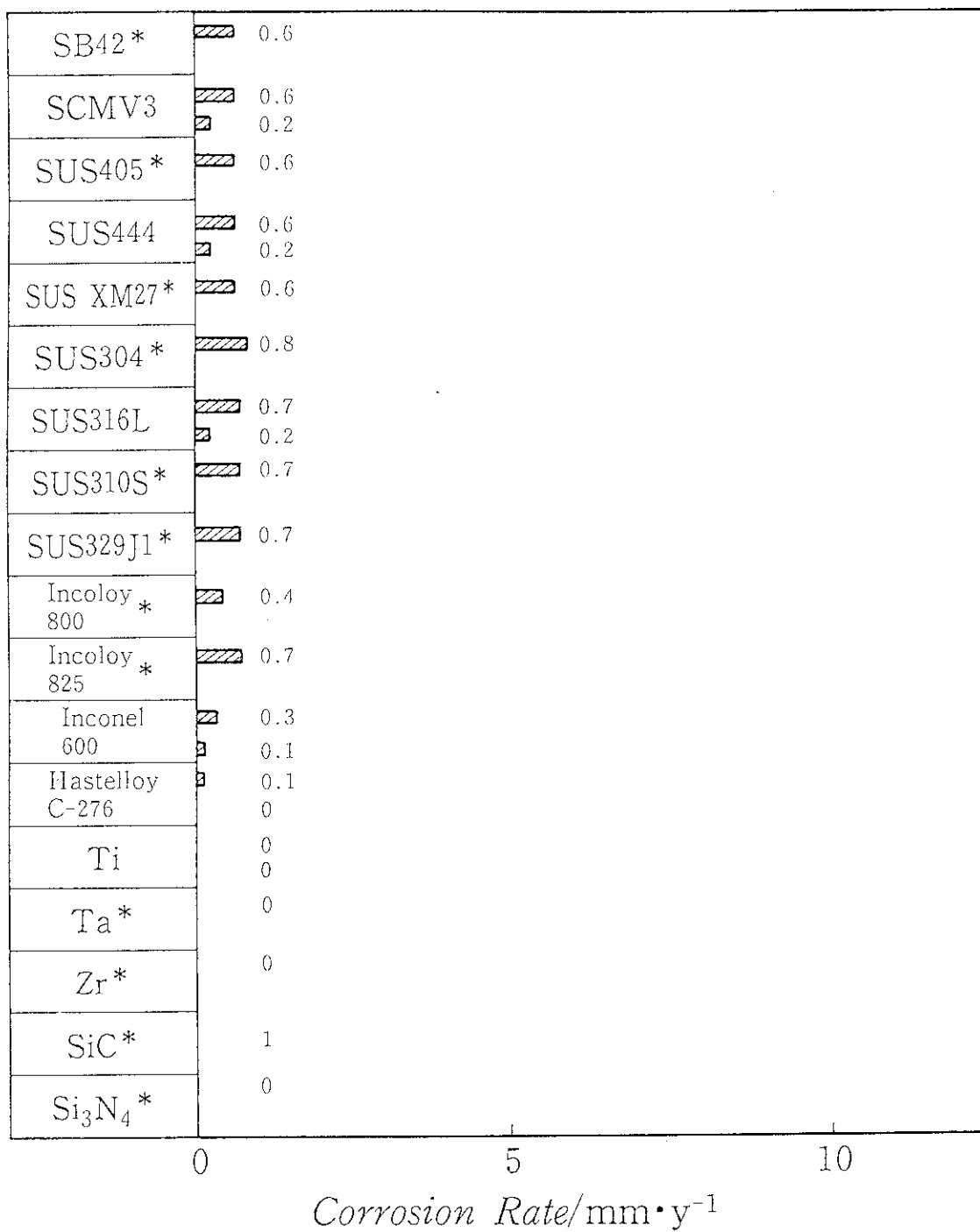


Fig. 5. 3(d) Corrosion rates in the simulated gaseous HI decomposer environment.

Molar ratio of HI/I<sub>2</sub>/H<sub>2</sub>O=1/1/6 at 673K.

Duration of exposure : 96hr(upper line), 1000hr(lower line).

\*) Only short term exposure test was carried out.

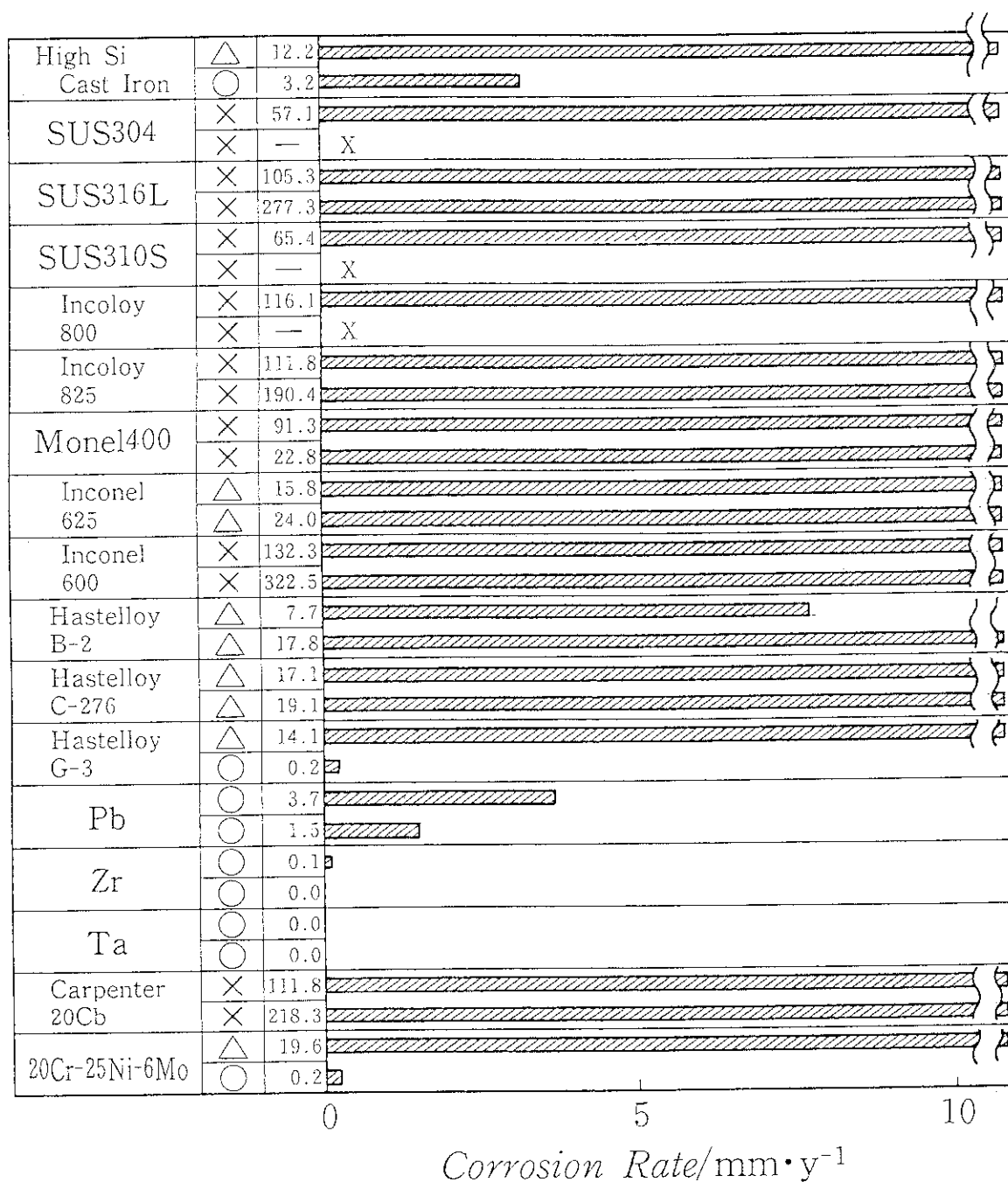


Fig. 5.4(a) Corrosion rates in the simulated sulfuric acid concentrator environment.  
40wt% H<sub>2</sub>SO<sub>4</sub>+1wt%HI+0.5wt%I soln. at boiling condition (393K).

Duration of exposure: 24hr.

The second column denotes the surface state of the test piece.

○: smooth, △: rough, ×: severely corroded.

The figure in the third column denotes the corrosion rate in mm y<sup>-1</sup>.

"X" means the test piece was dissolved.

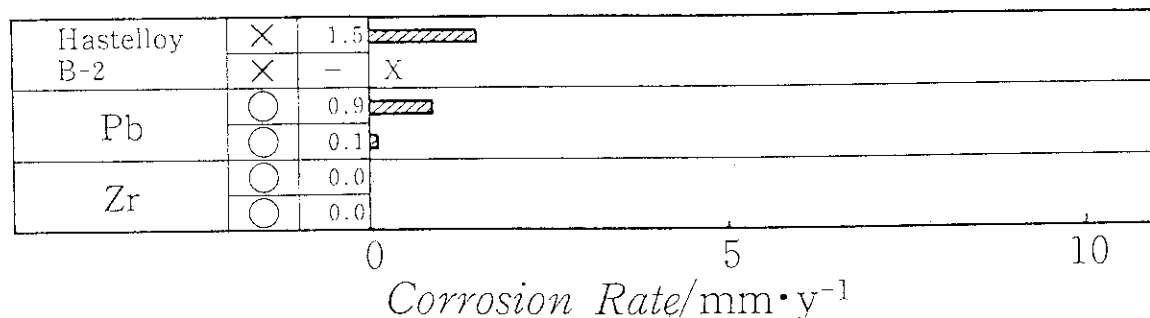


Fig. 5. 4 (b) Corrosion rates in the simulated sulfuric acid concentrator environment.  
40wt% H<sub>2</sub>SO<sub>4</sub>+1wt%HI+0.5wt%I<sub>2</sub> soln. at boiling condition (393K).

Duration of exposure : 800hr.

The second column denotes the surface state of the test piece.

○ : smooth, × : severely corroded.

The figure in the third column denotes the corrosion rate in mm y<sup>-1</sup>.

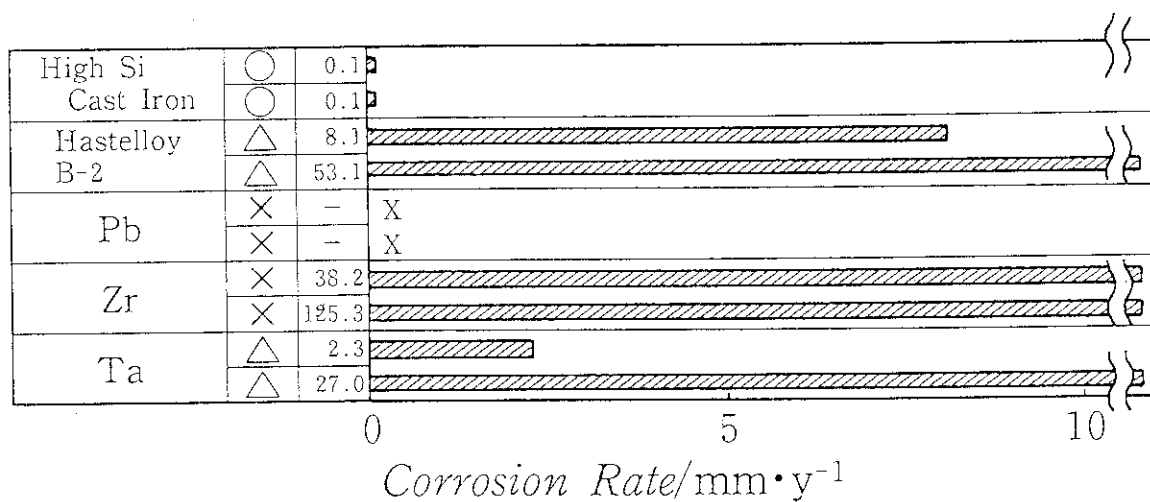


Fig. 5. 4 (c) Corrosion rates in the simulated sulfuric acid vaporizer environment.  
98wt% H<sub>2</sub>SO<sub>4</sub> soln. at boiling condition (593K).

Duration of exposure : 24hr.

The second column denotes the surface state of the test piece.

○ : smooth, △ : rough, × : severely corroded.

The figure in the third column denotes the corrosion rate in mm y<sup>-1</sup>.

"X" means the test piece was dissolved.

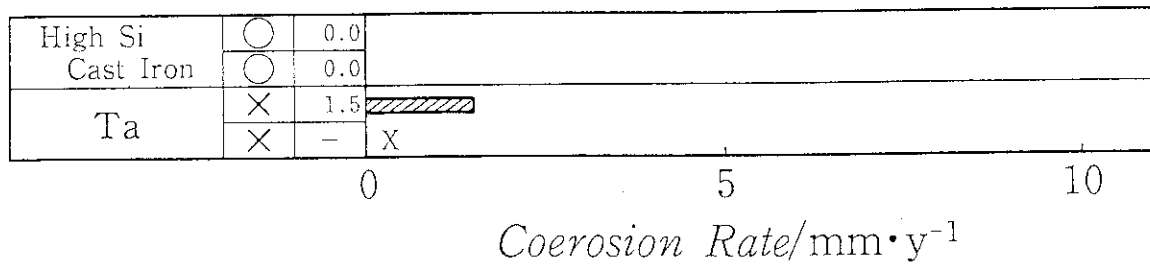


Fig. 5. 4 (d) Corrosion rates in the simulated sulfuric acid vaporizer environment.  
98wt%  $H_2SO_4$  soln. at boiling condition (593K).

Duration of exposure : 800hr.

The second column denotes the surface state of the test peace.

○ : smooth, × : severely corroded.

The figure in the third column denotes the corrosion rate in  $\text{mm y}^{-1}$ .

"X" means the test piece was decomposed.



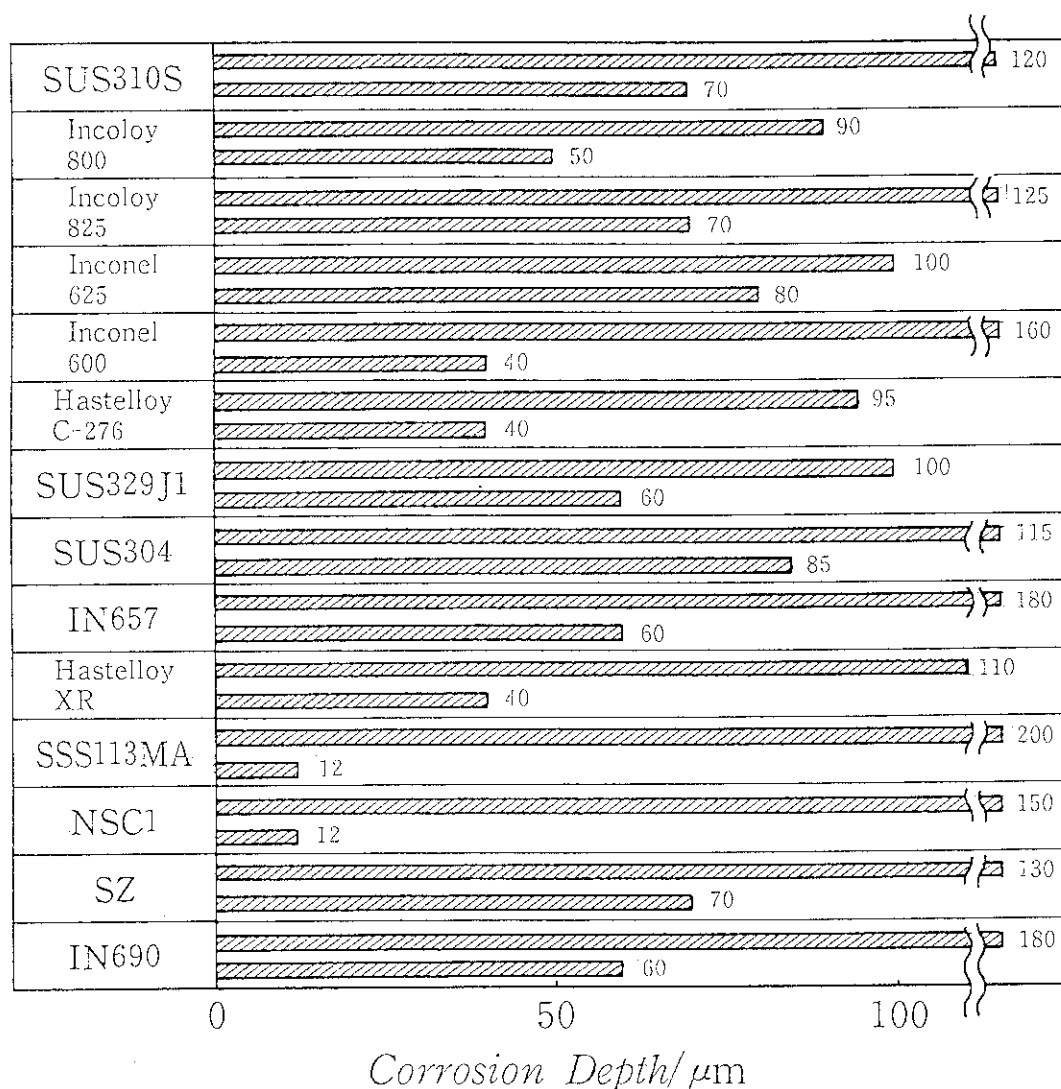


Fig. 5.5 Corrosion depths in the simulated  $\text{SO}_2$  decomposer environment.

Gaseous mixture by the 98wt%  $\text{H}_2\text{SO}_4$  vaporization (1123K).

Duration of exposure: 1000hr.

The upper and lower line corresponds to the result in the simulated environment before and after the catalyst zone, respectively.

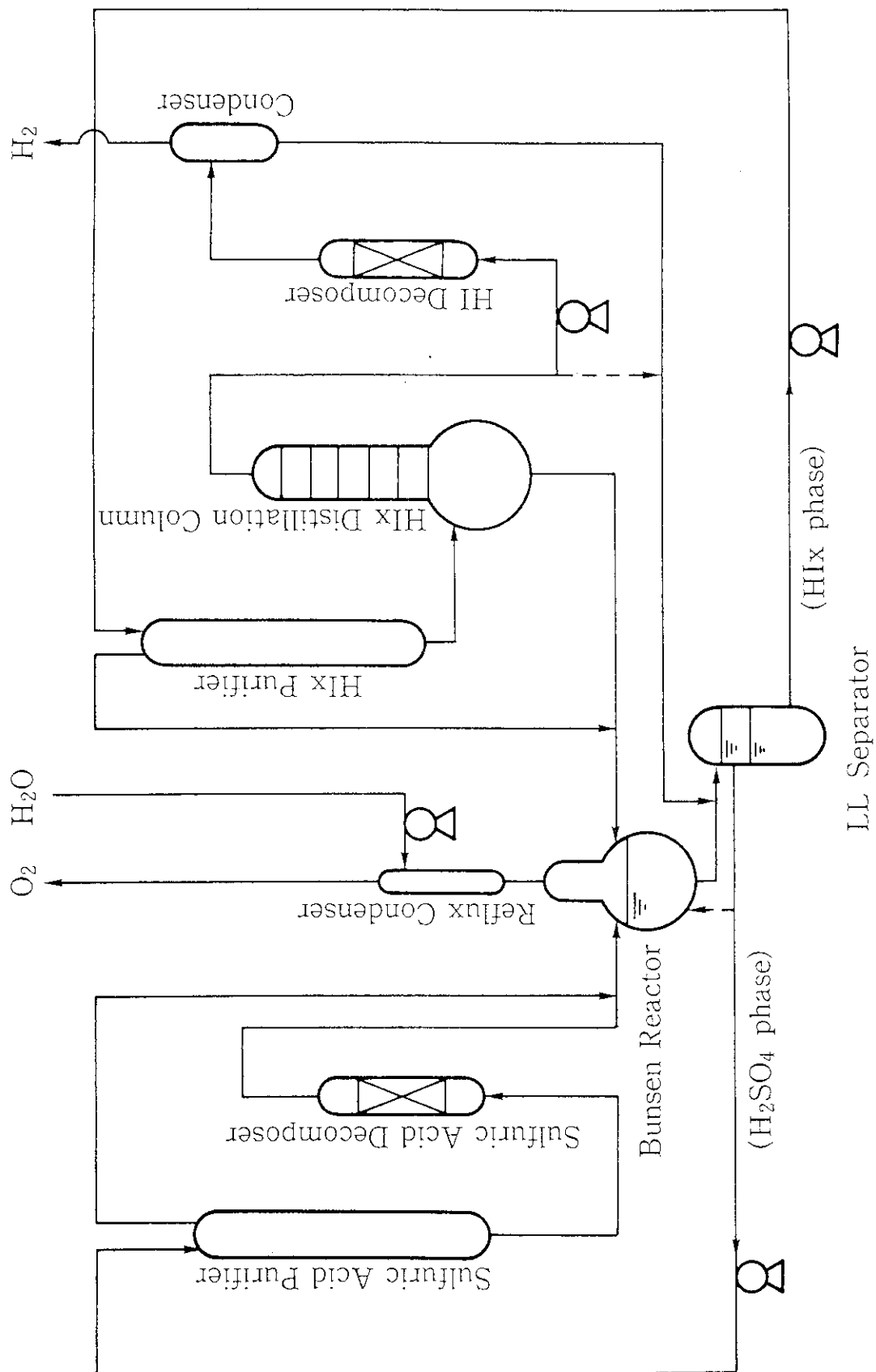


Fig. 6.1 Schematic flowsheet of the laboratory scale demonstration apparatus.

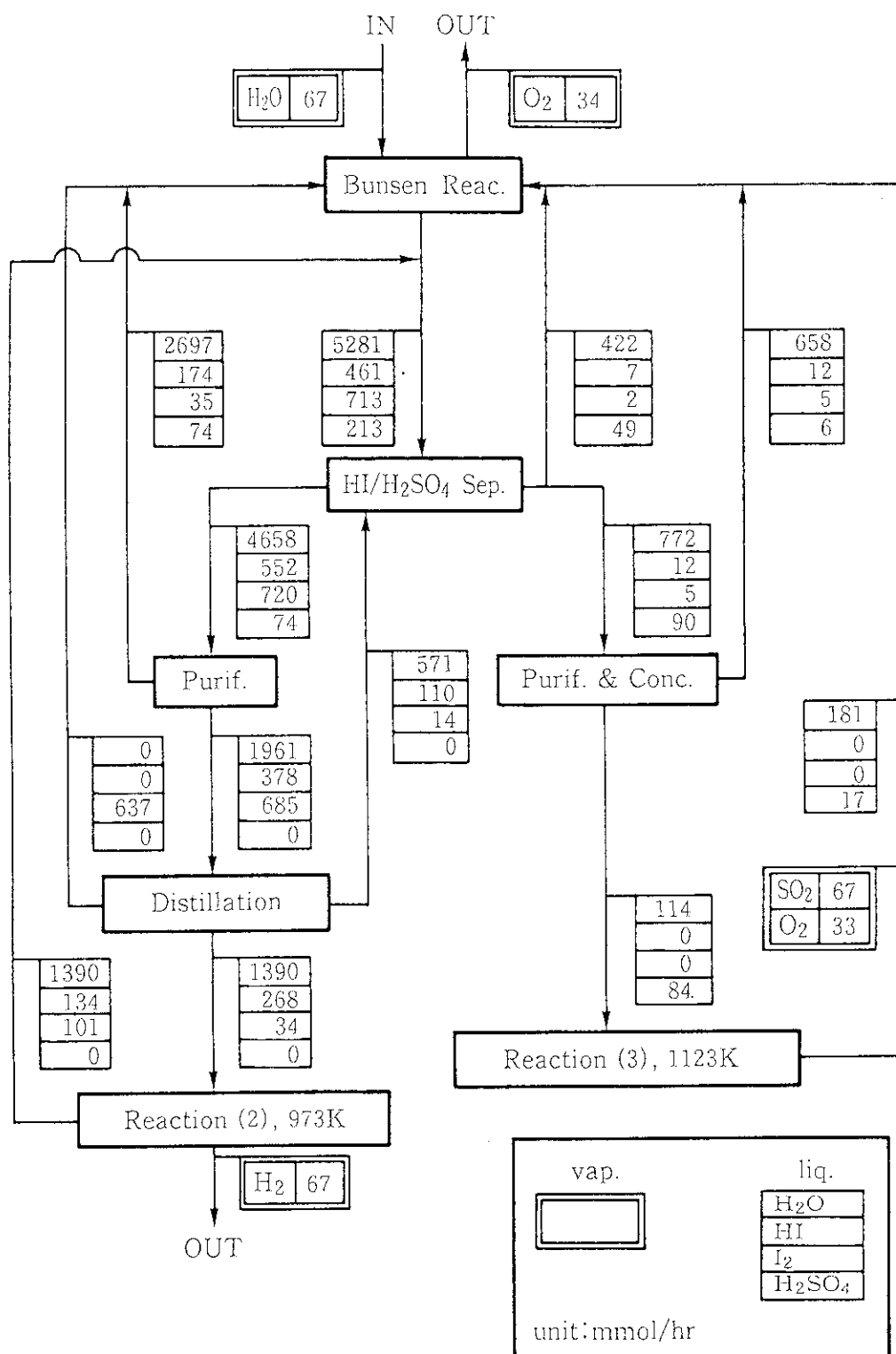


Fig. 6.2 Mass flow of the laboratory scale demonstration.

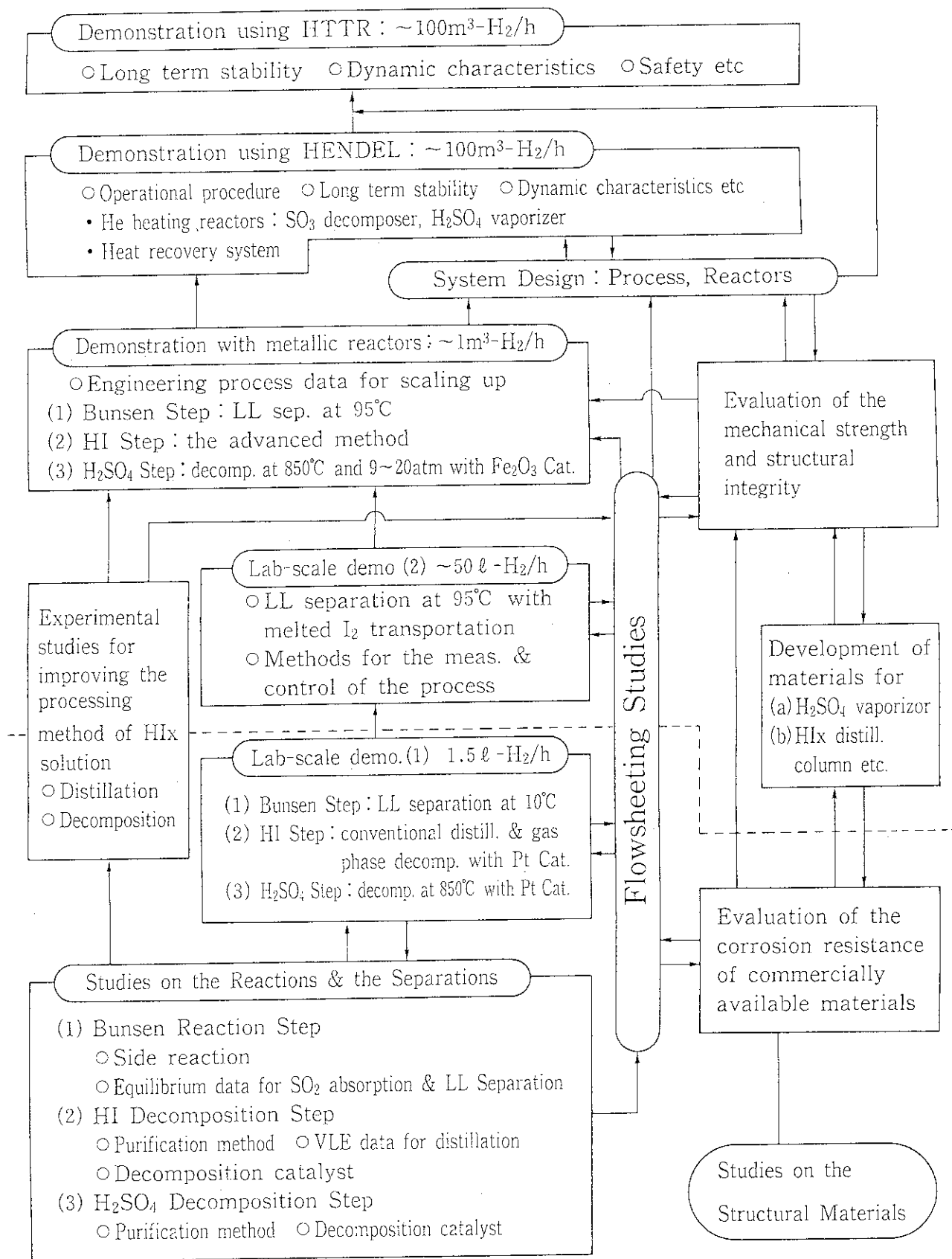


Fig. 7.1 R&amp;D scheme of the IS process